Cell, Vol. 98, 739–755, September 17, 1999, Copyright ©1999 by Cell Press

BDNF Regulates the Maturation of Inhibition and the Critical Period of Plasticity in Mouse Visual Cortex

Z. Josh Huang,*† Alfredo Kirkwood,‡ Tommaso Pizzorusso,§ Vittorio Porciatti,§ Bernardo Morales,‡ Mark F. Bear,*‖ Lamberto Maffei,§ and Susumu Tonegawa*†#

*Howard Hughes Medical Institute
†Center for Learning and Memory
Department of Biology and Department of Brain and Cognitive Science
Massachusetts Institute of Technology
Cambridge, Massachusetts 02139
‡Zanvyl Krieger Mind/Brain Institute
Johns Hopkins University
Baltimore, Maryland 21218
§Scuola Normale Superiore and
Istituto Neurofisiologia CNR
Pisa 56127
Italy
‖Department of Neuroscience
Brown University
Providence, Rhode Island 02912

Summary

Maturation of the visual cortex is influenced by visual experience during an early postnatal period. The factors that regulate such a critical period remain unclear. We examined the maturation and plasticity of the visual cortex in transgenic mice in which the postnatal rise of brain-derived neurotrophic factor (BDNF) was accelerated. In these mice, the maturation of GABAergic innervation and inhibition was accelerated. Furthermore, the age-dependent decline of cortical long-term potentiation induced by white matter stimulation, a form of synaptic plasticity sensitive to cortical inhibition, occurred earlier. Finally, transgenic mice showed a precocious development of visual acuity and an earlier termination of the critical period for ocular dominance plasticity. We propose that BDNF promotes the maturation of cortical inhibition during early postnatal life, thereby regulating the critical period for visual cortical plasticity.

Introduction

The neurotrophin family of growth factors, including nerve growth factor (NGF), brain-derived neurotrophic factor (BDNF), neurotrophin-3 (NT-3), and neurotrophin-4/5 (NT-4), have been implicated in the regulation of neuronal differentiation (Ghosh and Greenberg, 1995), axonal (Diamond et al., 1992; Cohen and Fraser, 1995) and dendritic (Cohen et al., 1991; McAllister et al., 1995) growth, and synapse formation (Cabelli et al., 1995; Wang et al., 1995). In addition, it has been reported that neurotrophins cause (Lohof et al., 1993; Kang and Schuman, 1995) and/or promote (Figurov et al., 1996; Huber et al., 1998) specific forms of synaptic plasticity during the postnatal period (reviewed in Lo, 1995; Thoenen, 1995; Bonhoeffer, 1996; Katz and Shatz, 1996). Since neurotrophin expression itself is strongly influenced by neuronal activity (Isackson et al., 1991; Castren et al., 1992; Patterson et al., 1992; Blochl and Thoenen, 1995), a reciprocal regulation between neurotrophin and neural activity may provide a means by which active neuronal connections and circuits are selectively strengthened.

Much effort has been directed toward testing the attractive hypothesis that a limited amount of neurotrophins in the postsynaptic target neurons may function as an activity-dependent retrograde messenger, which can act rapidly and locally to strengthen the more active presynaptic input (Maffei et al., 1992; reviewed in Thoenen, 1995). Such an "instructive" role of neurotrophins could underlie the activity-dependent synaptic competition thought to be crucial in synapse refinement processes, such as the segregation of LGN afferents into eye-specific patches in layer IV of the primary visual cortex (Goodman and Shatz, 1993). A prediction of this hypothesis is that an excess supply of target-derived neurotrophins should eliminate competition among thalamic inputs and therefore prevent the formation of ocular dominance columns or the physiological shift of ocular dominance following monocular deprivation (MD). Indeed, intracortical administrations of BDNF or its neutralizing agent, the trkB-IgG fusion protein, were shown to alter the formation (Cabelli et al., 1995, 1997) and plasticity (Galuske et al., 1996) of ocular dominance columns. Furthermore, cortical infusion of NT-4 rescued LGN neurons from the effect of MD (Riddle et al., 1995). These results are consistent with the notion that a ligand of TrkB, either BDNF and/or NT-4, acts directly on LGN axons and is involved in their activity-dependent competition for layer IV synaptic targets during ocular dominance segregation. However, alternative interpretations for these findings are plausible. For example, neurotrophins could affect LGN axons indirectly, via alterations in the dendritic morphology of cortical neurons, especially those in layer IV (McAllister et al., 1995). Neurotrophins may also support LGN axon terminal branching in a permissive and nonspecific manner, rather than in an activity-dependent manner.

More recently, a new role for neurotrophins in cortical development and plasticity has been postulated: the regulation of GABAergic inhibitory interneurons (Marty et al., 1997). In cortical cell culture, BDNF promotes interneuron neurite growth, stimulates the expression of GABA and several calcium-binding proteins (Collazo et al., 1992; Ip et al., 1993; Nawa et al., 1994; Widmer and Hefti, 1994; Marty et al., 1996), and regulates the strength of synaptic inhibition (Rutherford et al., 1997, 1998). These findings are potentially significant for understanding how neurotrophins might regulate experience-dependent synaptic modifications in visual cortex. Intracortical inhibition provides powerful control over activity-dependent synaptic plasticity (Artola and

#To whom correspondence should be addressed (e-mail: tonegawa@mit.edu).

Singer, 1987; Kirkwood and Bear, 1994; Hensch et al., 1998) and matures slowly in comparison with excitation (Blue and Parnevelas, 1983; Komatsu, 1983; Luhmann and Prince, 1991; Micheva and Beaulieu, 1997). It has been suggested that this developmental mismatch between inhibitory and excitatory processes provides a window of time—a critical period— when the organization of cortical circuitry can be strongly influenced by sensory experience (e.g., Kirkwood and Bear, 1994; Kirkwood et al., 1995; Micheva and Beaulieu, 1997). Indeed, the critical period for ocular dominance (OD) shift is prolonged (Cynader and Mitchell, 1980; Mower, 1991; Fagiolini et al., 1994) and the maturation of cortical inhibition delayed (Blue and Parnevelas, 1983; Benevento et al., 1992, 1995) when animals are reared in complete darkness. In addition, OD shift was prevented in mice deficient in an isoform of the GABA synthetic enzyme (GAD65) and was rescued by pharmacologically enhancing intracortical inhibition (Hensch et al., 1998). Since BDNF expression in the visual cortex is activity dependent and is reduced by dark rearing (Castren et al., 1992; Bozzi et al., 1995), these data together suggest that activity-dependent expression of BDNF regulates the maturation of inhibitory interneurons and, as a consequence, the duration of the postnatal critical period for experience-dependent plasticity. However, a causal link between BDNF expression, the maturation of the GABAergic interneurons, and the development and plasticity of the primary visual cortex has not been established.

The genetic approach in mice offers the opportunity for a combined molecular, anatomical, physiological, and behavioral analysis of the role of neurotrophins in activity-dependent developmental plasticity. Visual cortex in rodents, like those in carnivores and primates, is immature at the time of eye opening during the second postnatal week. The functional properties of the primary visual cortex, such as proper receptive field sizes, visual acuity, and orientation selectivity develop gradually during the subsequent weeks and reach adult level after the fifth week (Fagiolini et al., 1994). Importantly, these functional developments are profoundly influenced by manipulations of the visual input, with the best example being the ocular dominance shift following monocular deprivation during a well-defined critical period (Fagiolini et al., 1994; Gordon and Stryker, 1996).

Unfortunately, mice deficient for BDNF are grossly abnormal in the development of the peripheral nervous system and usually die within the first 2 weeks after birth (Ernfors et al., 1994; Jones et al., 1994). Therefore, to address the role of BDNF in cortical development, we took a different approach: we generated transgenic mice in which the postnatal rise of BDNF level in forebrain was genetically accelerated, using the promoter of α-calcium/calmodulin-dependent protein kinase II (αCaMKII). In these transgenic mice, we found a precocious termination of the critical period of ocular dominance plasticity and an accelerated development of visual acuity, with a time course that correlated with an accelerated maturation of GABAergic inhibitory circuitry and a precocious decline of in vitro visual cortical plasticity.

Results

Generation of Transgenic Mice Overexpressing BDNF in the Postnatal Forebrain

To construct the *BDNF* transgenic DNA vector, a Kozac sequence was first inserted in front of the translation initiation codon of the rat *BDNF* cDNA. This modified *BDNF* cDNA fragment was then linked to a 8.5 kb α*CaMKII* promoter (Mayford et al., 1995) and a SV40 intron and polyadenylation sequence (Figure 1A). A total of 16 transgenic founders were generated by pronuclei injection of the DNA construct. Of these, seven founders (more than 40%) died between 4 to 12 weeks of age. Six of the remaining nine lines expressed the *BDNF* transgene as determined by Northern blotting. Although the expression levels of the transgene varied among different lines, the spatial expression patterns were primarily restricted to the forebrain regions including the neocortex and hippocampus, with weak expressions in cerebellum only in high-expression lines (Figure 1B). In the highest expression line, A9, the total levels of *BDNF* mRNA (including the 1.6 kb and 4.0 kb endogenous and the 1.6 kb transgenic mRNAs) in adult neocortex and hippocampus was approximately 5-fold higher than those in wild-type mice (including both the 1.6 kb and 4.0 kb endogenous species). In two other lines (A92 and A10), the total levels of *BDNF* mRNA in adult neocortex and hippocampus were from 2- to 3-fold higher than those in wild-type littermates. We analyzed the highest expressor A9 further.

In the cerebral cortex of wild-type pups, *BDNF* mRNA was detected at very low levels at postnatal day 2 (P2). Expression gradually increased in the next few weeks, reaching a high level by 5 weeks of age (Figure 1C). In the cerebral cortex of A9 pups, the postnatal rise of *BDNF* expression was significantly accelerated. The expression of the *BDNF* transgene was already elevated at P2. By 3 weeks of age, *BDNF* mRNA levels in neocortex of A9 were already significantly higher than those in neocortex of 5-week-old wild-type mice (Figures 1C and 1D). At 5 weeks of age, total *BDNF* mRNA levels were approximately 3-fold higher in the neocortex of A9 mice compared to those in wild-type littermates (Figures 1C and 1D). The expression levels of various forms of the trkB receptors, assayed by Northern blotting, were not significantly altered in the *BDNF* transgenic mice (data not shown).

RNA in situ hybridization showed that *BDNF* overexpression was mostly restricted to the forebrain regions, including all areas of the neocortex and CA1, CA3, and dentate gyrus of the hippocampus (Figure 2A), the amygdala, and the striatum (data not shown). Within the primary visual cortex, the transgene expression was highest in the superficial layers (layers II and III), lower in the deep layers (layers V and VI), and still lower in layer IV (Figure 2A). This laminar pattern in the neocortex resembled those of the endogenous α*CaMKII* gene (Burgin et al., 1990) and the endogenous *BDNF* gene (Bozzi et al., 1995). In the transgenic mice, BDNF immunoreactivity (IR) was significantly stronger in the hippocampus (especially in CA3 where endogenous BDNF expression is low) and the cerebral cortex compared to those in

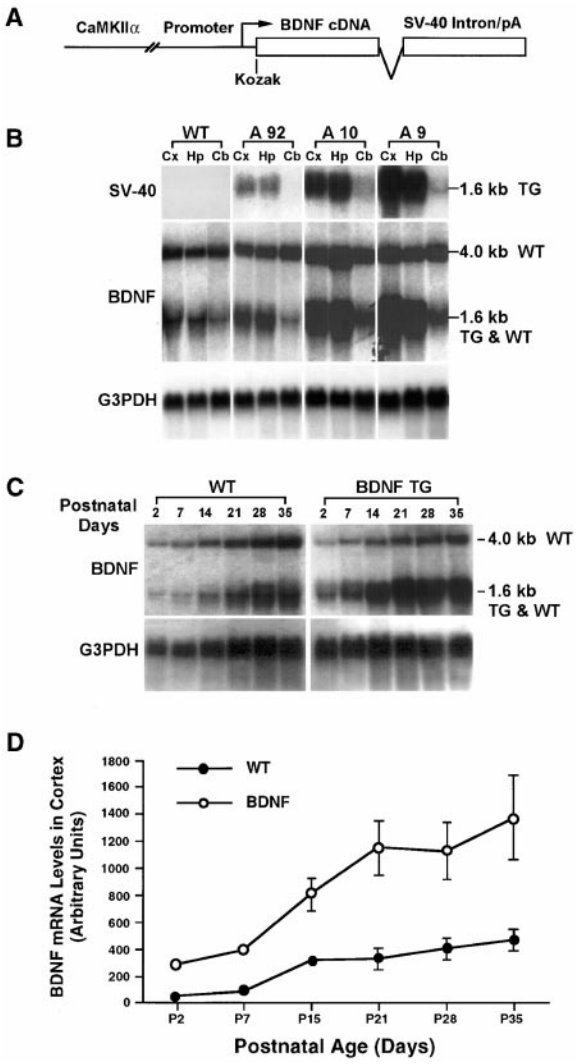

Figure 1. Expression of the *BDNF* Transgene

(A) Schematic representation of the αCaMKII-*BDNF* transgenic construct.

(B) Forebrain restricted expression of the *BDNF* transgene at low (A92), medium (A10), and high (A9) levels in three transgenic lines. Northern blot of approximately 20 μg of total RNA from the cerebral cortex (Cx), hippocampus (Hp), and cerebellum (Cb) of adult mice was hybridized with probes indicated at left. The SV-40 probe detects the 1.6 kb *BDNF* trangenic mRNA only. The *BDNF* probe detects both the transgenic and the two endogenous *BDNF* mRNA (1.6 kb and 4.0 kb). The G3PDH probe detects a ubiquitously expressed mRNA, which was used to adjust for the differences in the amount of RNA loaded in different lanes during quantitation.

(C) Postnatal developmental expression of the *BDNF* transgene in cerebral cortex. Northern blot of approximately 20 μg of total RNA from the cerebral cortex of mice at different postnatal ages were hybridized with probes indicated on the left.

(D) Quantification of total *BDNF* mRNA levels in the cerebral cortex at different developmental ages. Data were from two Northern blotting experiments as shown in (C). In wild-type mice, both the 1.6 kb and 4.0 kb *BDNF* mRNAs were included in quantitation. In the transgenic mice, both the endogenous (1.6 kb and 4.0 kb) and the transgenic (1.6 kb) *BDNF* mRNAs were included. Differences in the amount of RNA loaded in different lanes were adjusted using the G3PDH signals. See Experimental Procedures for details.

wild-type littermates (data not shown). In the adult primary visual cortex of wild-type mice (Figure 2B), endogenous BDNF IR was present in supragranular layers (layer II and III) and infragranular layers (layer V and VI). Only a few lightly labeled cells were present in layer IV. In contrast, there was a substantial increase of BDNF IR in all layers, including layer IV, of the primary visual cortex in the transgenic mice (Figure 2B). This was due to a marked increase both in the number of neurons positive for BDNF IR and in the intensity of BDNF IR in these neurons. BDNF IR was present both in the neuronal soma and neurites (Figure 2B and data not shown).

Endogenous BDNF has been shown to be expressed in pyramidal neurons but not GABAergic interneurons in rodent visual cortex (Cellerino et al., 1996; Gorba and Wahle, 1999). To determine whether the overexpressed BDNF was mainly in the pyramidal neurons or GABAergic interneurons, brain sections were imaged using confocal microscopy for colocalization of BDNF with either parvalbumin (Pv) or αCaMKII. Parvalbumin is a calcium-binding protein expressed in approximately 50% of the GABAergic neurons (Gonchar and Burkhalter, 1997), and αCaMKII is restricted to the pyramidal neurons (Liu and Jones, 1996) in rodent visual cortex. The great majority of BDNF-overexpressing neurons were also positive for αCaMKII IR (Figure 2D). Out of 80 BDNF-expressing neurons imaged, 76 were positive for CaMKIIα IR. These neurons were frequently surrounded by Pv-positive boutons of GABAergic interneurons (Figure 2C). On the other hand, the great majority of Pv neurons were negative for BDNF IR (Figure 2C). Out of 56 Pv neurons imaged, only 2 contained very faint BDNF IR in cell soma. Therefore, as is the case for endogenous BDNF, transgenic BDNF overexpression is predominantly restricted to pyramidal neurons in the visual cortex.

Since the *BDNF* transgene might alter perinatal development of the brain, we examined Nissl-stained coronal brain sections (Figure 2E). No gross alterations in the forebrain structure were detected. The cortex was of normal thickness, and no abnomalities in lamination were seen. No significant difference in neuronal cell density in the primary visual cortex was detected between wild-type and transgenic mice. In a 250 μm × 250 μm area that covered layers II–IV, the neuron counts for adult wild-type and trangenic animals were 210 ± 27 (n = 9 counts from three mice, 20 μm thick sections) and 230 ± 15 (n = 9 counts from three mice, 20 μm thick sections), respectively. The transgenic animals were healthy, exhibited no obvious behavioral defects, and had a normal life span.

Accelerated Maturation of GABAergic Innervation and Inhibition in the Primary Visual Cortex of *BDNF* Transgenic Mice

To examine the effect of BDNF overexpression on the development of the GABAergic system, we first analyzed the expression of GAD65 (an isoform of the glutamic acid decarboxylase) and that of parvalbumin in developing primary visual cortex. GAD65 is primarily localized in axonal terminals and presynaptic boutons and is associated with synaptic vesicles and plasma membranes of GABAergic neurons in adult brain (Reetz et al., 1991; Esclapez et al., 1994; Shi et al., 1994). At

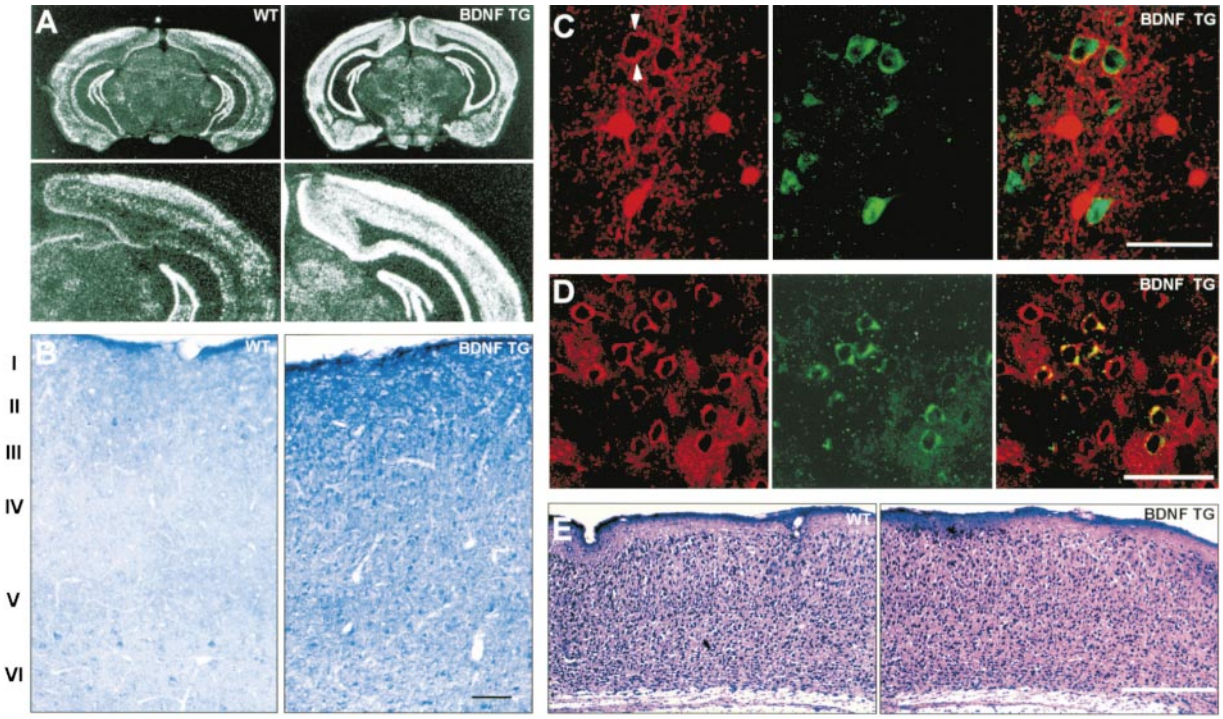

Figure 2. Spatial and Cellular Expression Pattern of the *BDNF* Transgene in Line A9

(A) Spatial expression of the *BDNF* transgene revealed by in situ hybridization. Coronal brain sections from 4-week-old transgenic (right) and wild-type mice (left) hybridized with a *BDNF* oligo nucleotide probe that detects both the endogenous and transgenic *BDNF* mRNA.

(B) Expression of the BDNF protein in the visual cortex in adult transgenic and wild-type mice. Coronal sections from transgenic and wild-type mice were reacted with a BDNF polyclonal antibody. Due to the limited availability, the antibody was used at one-fifth of the dilution as in Yan et al. (1997). Cortical laminae are indicated at left. Note BDNF overexpression in all layers, including layer IV, in visual cortex of transgenic mice. Bar, 80 μm.

(C) BDNF overexpression was absent in GABAergic interneurons. Coronal sections of visual cortex of transgenic mice were double-labeled with antibodies against parvalbumin (red, left panel) and BDNF (green, middle panel) and imaged for colocalization (right panel) using confocal microscopy. White arrowheads indicate parvalbumin-positive boutons. Pial surface is to the right. Bar, 50 μm.

(D) BDNF overexpression was restricted to pyramidal neurons. Coronal sections of visual cortex of transgenic mice were double-labeled with antibodies against CaMKIIα (red, left panel) and BDNF (green, middle panel) and imaged for colocalization (yellow, right panel) using confocal microscopy. Pial surface is to the right. Bar, 50 μm.

(E) The laminar pattern in the visual cortex of the transgenic mice is normal. Coronal sections from adult transgenic and wild-type mice were processed by Nissl stain. Bar, 400 μm.

these sites, the conversion of the apoenzyme to holoenzyme (the active form of GAD65) can be regulated by local influx of cofactors (e.g., pyridoxal 5′phosphate) and has an immediate influence on synaptic activity through the local synthesis of GABA (reviewed in Martin and Rimvall, 1993).

Previous work has shown that GABA and GAD can be detected in the occipital cortex of rodents at a late embryonic stage (Wolff et al., 1984; Del Rio et al., 1992). At birth, both GABA and GAD are initially localized in the cell soma and gradually proceed to dendrites and axonal terminals during the first few postnatal weeks (Wolff et al., 1984; Dupuy and Houser, 1996). The mature pattern of GABAergic innervation in the visual cortex is characterized by puncta-ring structures composed of GAD65-immunoreactive presynaptic boutons surrounding the soma and proximal dendrites of their target neurons. Such a pattern is not fully established until after the fourth postnatal week (Wolff et al., 1984).

In mature (P35) wild-type mice, GAD65 IR was observed in all layers of the primary visual cortex (e.g., Figure 3A, P35 and data not shown) and was concentrated in axon terminals and presynaptic boutons of GABAergic interneurons. Very few cell somata were labeled with GAD65, and when labeled, the soma staining was always weak. Distinctive puncta rings were prominent in all cortical layers (Figure 3A, P35 and data not shown). GAD65-positive puncta were also present throughout the neuropil region. In contrast, the pattern of GAD65 IR was markedly different in visual cortex of P12 wild-type pups (Figure 3A, P12). Many somata were strongly labeled, while the GAD65 IR in axon terminals was weak and diffuse. Few if any puncta rings were observed. Over the course of the next 2 weeks, the patterns of GAD65 expression slowly matured to resemble that of the adult mice. However, even at P24, many puncta rings were still incomplete and weak, especially in layer III and layer IV (Figure 3A).

In *BDNF* transgenic pups (Figure 3A, P12), the GAD65 IR pattern was similar to that in the wild-type littermates. Over the next 2 weeks, however, the progression to an adult-like pattern was significantly accelerated in the *BDNF* transgenics. At P21, prominent puncta rings were already detected (Figure 3A, P21), and by P24, adult-like puncta rings were abundant in all layers of the primary visual cortex of the transgenic mice. At P21 and

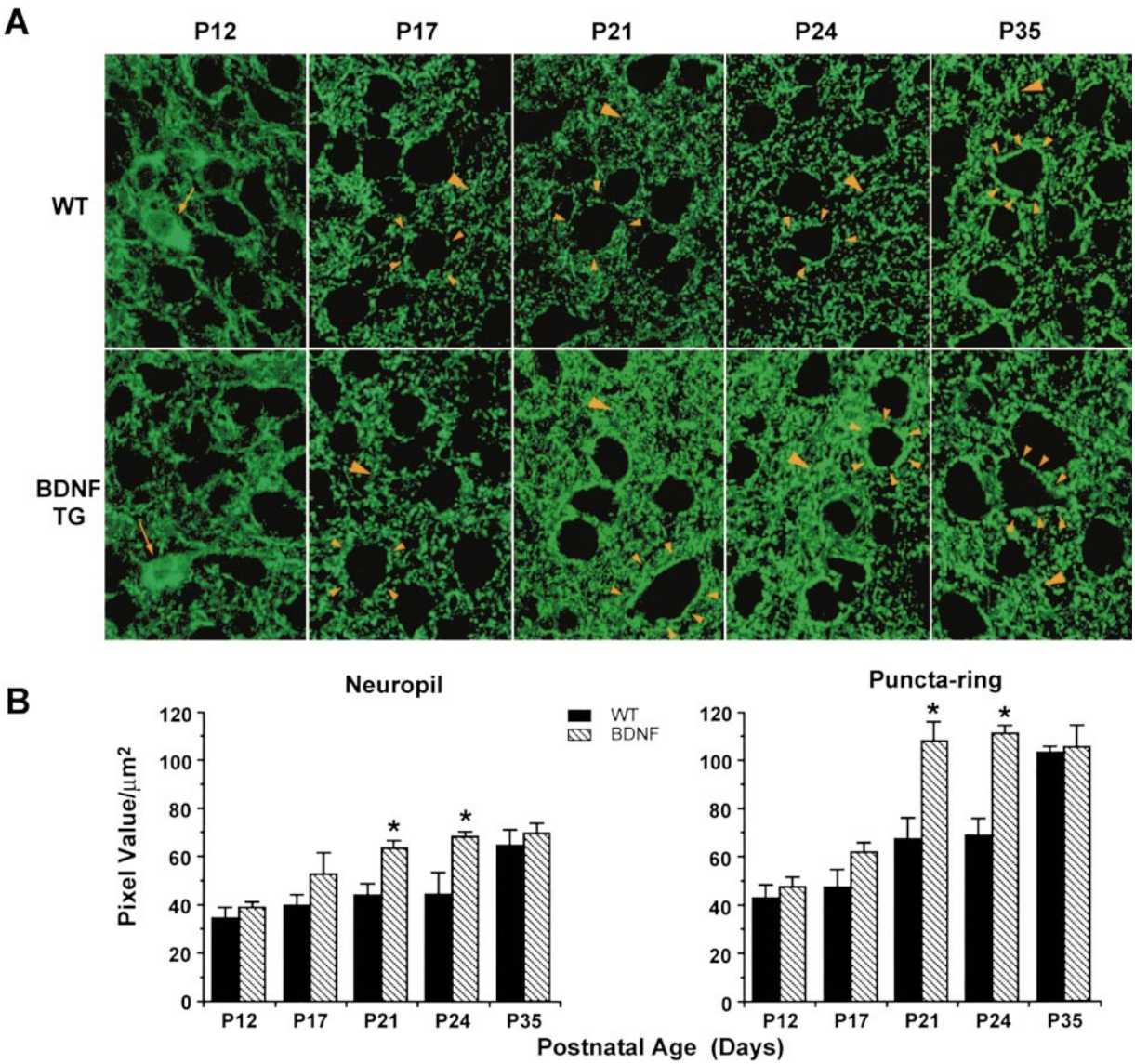

Figure 3. Accelerated Maturation of the GAD65 Expression in Layers III and IV in the Primary Visual Cortex of the *BDNF* Transgenic Mice

(A) Coronal brain sections (20 μm) containing the primary visual cortex from wild-type and transgenic mice at different postnatal ages (indicated at the top) were reacted with a monoclonal antibody against GAD65 and visualized with fluorescein-conjugated anti-mouse IgG. Arrows in P12 panels indicate GAD65 localization in the cell soma of GABAergic interneurons. Small arrowheads indicate GAD65 localization in the presynaptic boutons of GABAgergic interneurons surrounding the soma of their postsynaptic targets. These boutons form puncta rings (small arrowheads) in the more mature visual cortex. Large arrowheads indicate GAD65 localization in the presynaptic boutons of GABAgergic interneurons in the neuropil region of the visual cortex. Note the early appearance of prominent puncta rings in transgenic mice at P21 and P24. Bar, 15 μm.

(B) Quantification of GAD65 expression in the presynaptic boutons of GABAgergic interneurons in the neuropil region (left) and around the soma of the target neurons (right). Star indicates a significant difference between wild-type and transgenic mice (one-way ANOVA, $p < 0.01$). See Experimental Procedures for details on confocal microscopy and quantitation.

P24, the punctate staining in the neuropil region was also more intense and larger in size in trangenics as compared to that of wild-type littermates (Figure 3A). Quantification using confocal microscopy confirmed our visual impression and revealed that the enhancement of GAD65 IR in the transgenic mice compared to wild-type littermates was greater in puncta rings than that in the neuropil region (Figure 3B). Between P35 and P39, quantitation revealed no significant difference in GAD65 IR between transgenic and wild-type mice (Figure 3B). We also carried out the analysis using the peroxidase-anti-peroxidase method to visualize GAD65 at P12, P21, and P39 and reached similar conclusions (data not shown).

Parvalbumin-positive (Pv) interneurons in the cortex have been identified as basket cells or chandelier cells that innervate the soma or axon initial segments of pyramidal neurons (Del Rio et al., 1994). The onset of parvalbumin expression in the rodent visual cortex does not start until P12 (Del Rio et al., 1994). In the following 2

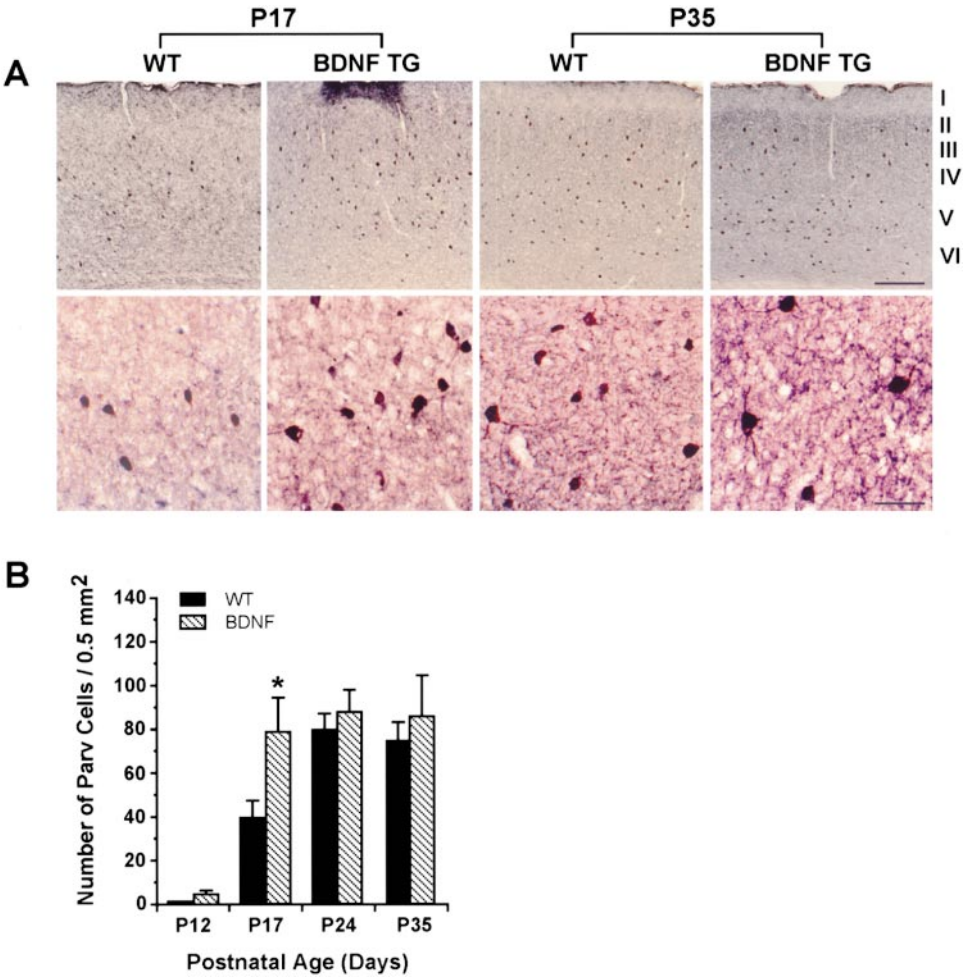

Figure 4. Accelerated Maturation of the Parvalbumin-Containing Interneurons in the Visual Cortex of the *BDNF* Transgenic Mice

(A) Coronal brain sections (20 μm thick) from wild-type and transgenic mice at two postnatal ages (indicated at the top) were reacted with a monoclonal antibody against parvalbumin and visualized with peroxidase method (ABC kit, Vector). Cortical laminae are indicated at right. Note that at P17, parvalbumin neurons in the transgenic mice have larger soma size compared to those from wild-type littermates (lower panels). Bars, 200 μm in upper panel and 50 μm in lower panel.

(B) Densities of parvalbumin-containing interneurons in the visual cortex of *BDNF* and wild-type mice at different postnatal ages. Star indicates a significant difference between wild-type and transgenic mice (single-factor ANOVA, $p < 0.01$). See Experimental Procedures for details on quantitation.

weeks, the number of Pv interneurons rises substantially. They spread from layer V to superficial and deep layers, and they reach the adult pattern in the fourth postnatal week. There is also a substantial increase in their soma size, neurite arborization, and synaptic innervation (Del Rio et al., 1994).

In *BDNF* transgenic mice, the maturation of Pv interneurons was accelerated (Figure 4). At P17, the number of Pv interneurons was about half of the adult level in the wild-type mice. In *BDNF* transgenics of the same age, the number of Pv interneurons had already reached the adult level (Figure 4B). In addition, Pv interneurons in the transgenic mice had larger soma sizes and more extensive neurite arborizations than those in the wild-type littermates (P17, Figure 4B). In the mature visual cortex, however, the density of Pv neurons was similar between transgenic and wild-type mice, and there was no significant difference in soma size and the exuberance of neurites detected by light microscopy (P35, Figure 4). These results corroborate the GAD65 data described above and suggest that the neurochemical maturation of GABAergic interneurons in the visual cortex is also accelerated in the *BDNF* transgenic mice.

To examine whether the accelerated morphological and neurochemical maturation of GABAergic interneurons was accompanied by a correlated increase in the strength of synaptic inhibition, we measured inhibitory postsynaptic responses in visual cortical slices from juvenile (P23-P26) wild-type and *BDNF* transgenic mice. In these experiments, we determined the amplitude of the maximal inhibitory postsynaptic currents (IPSCs) in layer III pyramidal neurons evoked by layer IV stimulation. IPSCs were isolated by holding the membrane potential at 0 mV, which is the reversal potential for AMPA

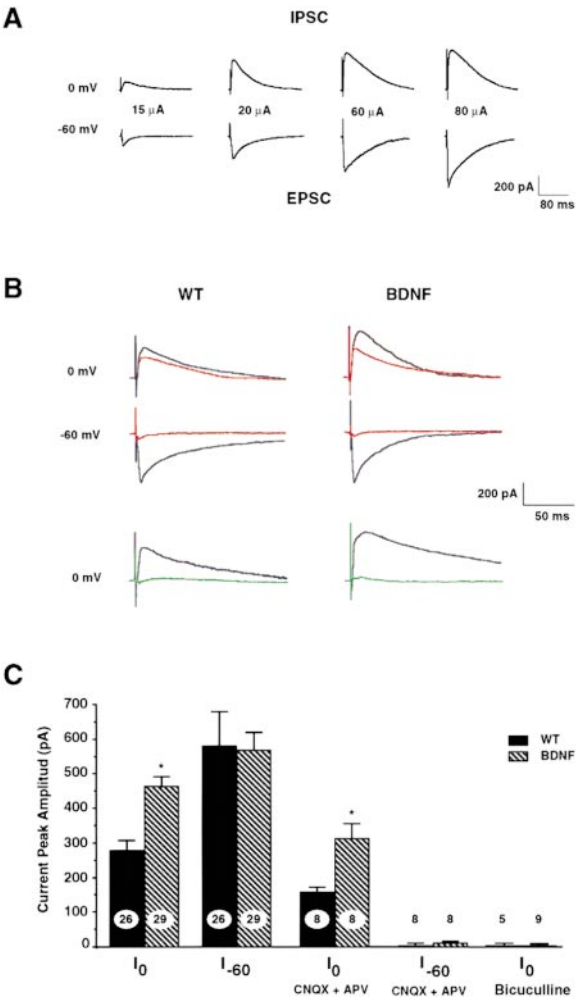

Figure 5. IPSCs Recorded in Layer II/III Pyramidal Neurons Were Larger in Slices from Juvenile (P23–P26) *BDNF* Transgenic Mice

(A) Relationship between stimulus intensity and the amplitude of IPSCs (measured at 0 mV) and EPSCs (measured at −60 mV). The IPSCs reached saturation when stimulus intensity was at 80 μA, and the amplitude of this maximal response was used as a measure of the strength of inhibition

(B) Examples of maximal IPSCs (top and bottom traces) and EPSCs (middle traces) recorded from slices prepared from *BDNF* mice (right) and wild-type mice (left). Traces in black were recorded in normal ACSF; traces in red were recorded in ACSF in the presence of 10 μM CNQX and 100 μM APV; and traces in green were recorded in the presence of 5 μM bicuculline.

(C) Summary graph showing mean IPSC and EPSC amplitudes in normal ACSF, and in ACSF with the presence of CNQX + AP5 or bicuculline. IPSCs were partially inhibited by the addition of CNQX + AP5 and completely inhibited by bicuculline. EPSCs, in contrast, were completely inhibited by CNQX + AP5. Asterisks denote significant differences ($p < 0.05$, one-way ANOVA) between *BDNF* mice and wild-type mice.

and NMDA receptors (0.5 ± 3.5 mV, n = 10 in *BDNF* transgenic mice; 0.5 ± 4.90 mV, n = 4 in wild-type mice). Likewise, EPSCs were isolated by holding neurons at −60 mV, which was close to the IPSC reversal potential (−62.1 ± 1.0 mV, n = 8 in *BDNF* transgenic mice; −61.63 ± 1.45 mV, n = 8 in wild-type mice). The stimulus intensity to recruit a saturating IPSC (Figure 5A) was similar in slices from *BDNF* (91 ± 18 μA, n = 29) and wild-type (107 ± 21 μA, n = 29) mice. However, the amplitude of this maximal IPSC (Figures 5B and 5C) was consistently and significantly larger ($p < 0.05$) in the *BDNF* transgenics (462 ± 29 pA, n = 29) than that in their wild-type littermates (279 ± 29 pA, n = 26). In contrast, there was no difference in EPSC amplitudes (619 ± 116 pA, n = 22 in *BDNF* transgenic mice; 564 ± 52 pA, n = 26 in wild-type mice) nor in whole-cell capacitances (111 ± 15 pF, n = 11 in *BDNF* transgenics; 112 ± 10 pF, n = 11 in wild-type mice), suggesting that the increase in the IPSCs did not result from an increase in cell size.

We also confirmed the above observation in pharmacologically isolated IPSCs, which were recorded in the presence of 10 μM CNQX and 100 μM APV to block AMPA and NMDA receptors, respectively. The glutamatergic antagonists completely eliminated the EPSCs recorded at −60 mV and reduced somewhat the IPSCs, possibly by eliminating the polysynaptic recruitment of synaptic inhibition (Figures 5B and 5C). Nevertheless, the IPSCs were still larger in slices prepared from *BDNF* transgenic mice (312 ± 45 pA, n = 8) than those in slices from wild-type mice (157 ± 16 pA, n = 8). Taken together, the results indicate that GABAergic inhibition in the visual cortex is stronger in *BDNF* transgenic mice at these young ages (P23–P26). These data are consistent with the accelerated maturation of GAD65 IR in the visual cortex of the transgenic mice (see above).

Accelerated Developmental Decline of White Matter–Evoked, Layer III LTP in *BDNF* Transgenic Mice

In order to determine the effect of an accelerated maturation of cortical inhibition on the activation of cortical synapses by afferent input, we turned to an in vitro model of visual cortical development and plasticity. Long-term potentiation of layer III synaptic responses can be induced with theta burst stimulation (TBS) applied to the white matter–layer VI border (WM→III LTP) in visual cortical slices prepared from young animals, but not from adults (Perkins and Teyler, 1988; Kato et al., 1991; Kirkwood et al., 1995). The "critical period" for WM→III LTP coincides with the critical period for ocular dominance shift in rodents, and both critical periods can be prolonged by rearing animals in the dark (Kirkwood et al., 1995). The inability to induce WM→III LTP in the adult is thought to reflect the maturation of intracortical inhibitory circuitry (Kirkwood and Bear, 1994). Consistent with this notion, WM→III LTP can be restored in slices from adult animals if GABAA-mediated inhibition is reduced (Artola and Singer, 1987; Kirkwood and Bear, 1994). We therefore reasoned that the earlier maturation of the cortical inhibitory circuitry in *BDNF* transgenic mice might lead to an earlier reduction in the activation of cortical synapses by afferent input and therefore an earlier developmental decline of WM→III LTP.

Figures 6A and 6B shows a comparison of WM→III LTP in P23-P26 *BDNF* transgenic mice and their wild-type littermates. In wild-type mice, TBS applied to the WM induced substantial LTP (122.2% ± 4.7% of baseline at 30 min after TBS; n = 10), as expected for animals in this age range. In contrast, TBS induced very little LTP in *BDNF* transgenics. After an initial potentiation,

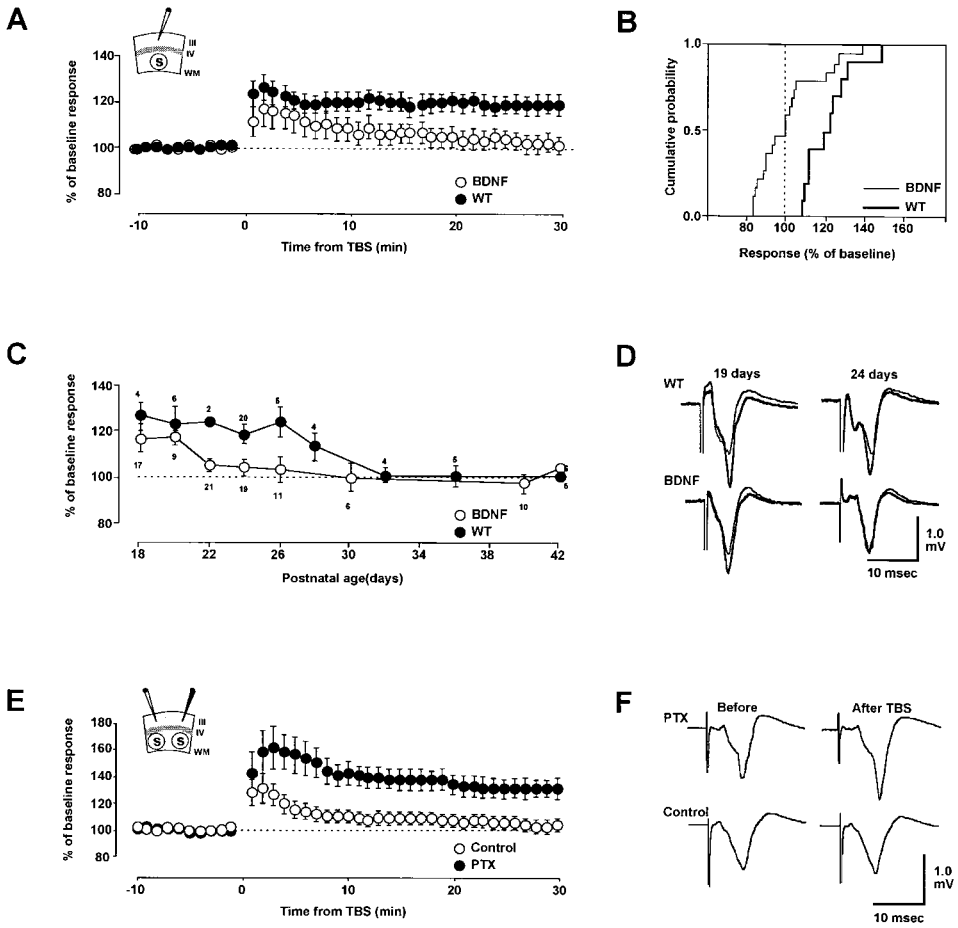

Figure 6. Accelerated Developmental Decline of WM→III LTP in Visual Cortex of *BDNF* Transgenic Mice

(A and B) A "blind" study showing that LTP in layer II/III induced with theta burst stimulation (TBS) of the white matter (WM→III LTP) is less pronounced in *BDNF* transgenic mice compared to those in their wild-type littermates at ages P23–P26. (A) The average time course of the changes in layer III field synaptic potential (FP) amplitude after TBS ("S" in the slice diagram) of the WM in wild-type and *BDNF* transgenic mice. (B) Cumulative probability distribution of the changes induced by TBS in slices obtained from *BDNF* transgenics (thin line) and wild-type mice (thick line). The percentage change over the baseline was measured at 30 min after conditioning. Data were from same experiments as in (A).

(C and D) Accelerated developmental decline of WM→III LTP in *BDNF* transgenic mice. (C) Postnatal age-dependent changes in the magnitude of WM→III LTP measured at 30 min after TBS was applied to the white matter. Each point represents the average (± SEM) of data pooled from two consecutive days. The number of slices averaged for each point is indicated above (for wild type) or below (for *BDNF* mice) the symbols. (D) Examples of WM→III LTP in *BDNF* and wild-type mice obtained at two different ages (19 and 24 days). Traces are averages of four consecutive field responses recorded before (thin lines) and 30 min after TBS applied to the white matter (thick lines).

(E and F) Local blockade of GABAA synaptic inhibition rescued the WM→III LTP in slices prepared from juvenile *BDNF* transgenic mice (P23–P25). Field potentials were simultaneously recorded at two sites of the same slice using micropipettes filled with normal ASCF (open circles) or with ACSF plus 1–5 mM picrotoxin (filled circles). (E) Time course of the effect of TBS. (F) Traces from representative experiments. Each trace is an average of four consecutive field responses recorded before (left) and 30 min after TBS applied to the white matter (right) in the presence (upper) or absence (lower) of PTX.

the responses rapidly declined back to the baseline level (101.3% ± 3.7% at 30 min after TBS, n = 19). The difference between transgenics and wild-type mice was significant ($p < 0.01$, t test). This difference in LTP was not explained simply by a difference in response size: the average half-maximal field potential (FP) was similar in *BDNF* transgenic (1.31 ± 0.09 mV, n = 46) and in wild-type mice (1.41 ± 0.10 mV, n = 37; p = 0.441). Subsequently, we measured the extent of WM→III LTP at different stages of early postnatal development. The results, shown in Figures 6C and 6D, indicate that the magnitude of LTP (30 min after TBS) undergoes a sharp decline between the fourth and the fifth postnatal weeks in wild-type mice. In *BDNF* transgenic littermates, this decline in LTP amplitude occurred 1 week earlier. Two-way ANOVA confirmed a significant interaction between the effects of age and genotype on LTP ($F [17, 15] = 3.7$, $p < 0.001$).

If the precocious decline in WM→III LTP was explained by accelerated maturation of inhibition, it should be possible to "rescue" WM→III LTP by blocking intracortical inhibition in slices derived from juvenile *BDNF* transgenic mice. To test this idea, we performed the experiment illustrated in Figures 6E and 6F. Slices were prepared from P23-P25 *BDNF* transgenic mice, and two independent stimulation-recording sites were studied

simultaneously. The recording electrode at one site was filled with ACSF containing the GABAA antagonist picrotoxin (2–5 mM). We have previously shown that this method blocks inhibition locally but prevents runaway excitation (Kirkwood and Bear, 1994). The other recording electrode was filled with normal ACSF and was used to record control responses. In each experiment ($n = 10$), baseline stimulation and TBS conditioning were delivered simultaneously to both sites. We found that WM→III LTP was consistently evoked at the site recorded with the picrotoxin electrode (138.4% ± 8.4%), but not at the control site (103.4% ± 4.6%; $p < 0.05$). These findings showed that *BDNF* transgenic mice at P23–P25 can support WM→III LTP when inhibition was reduced. The data are consistent with the notion that the earlier decline of WM→III LTP in BDNF overexpressing mice results from an early maturation of GABAergic inhibitory circuitry.

Precocious Termination of Critical Period for Ocular Dominance Plasticity in *BDNF* Transgenic Mice

What might be the functional consequences of an accelerated maturation of cortical inhibitory circuitry and a precocious decline of WM→III LTP on ocular dominance plasticity in the visual cortex? To address this question, we measured the degree of ocular dominance shift following a brief period of monocular deprivation (MD) applied to wild-type and *BDNF* transgenic mice at different postnatal ages, by recording local visual-evoked potentials (VEPs) from the binocular region of the primary visual cortex. VEPs represent the integrated response of a population of neurons to patterned visual stimuli and have been used to measure visual acuity, contrast sensitivity, cortical retinotopy, and binocularity in rodents (Porciatti et al., 1999).

In nondeprived wild-type adult mice, the amplitude of VEPs induced by stimulation of the contralateral eye was larger than that induced by stimulation of the ipsilateral eye by a factor of 3 (Figures 7A–7C). Such contralateral bias in VEPs amplitude is mainly due to the predominance of crossed fibers in mouse retinal projections (e.g., Drager and Olsen, 1980). The data are in agreement with the contralateral bias of ocular dominance distribution of single units in binocular visual cortex (Drager, 1975; Gordon and Stryker, 1996). In nondeprived adult *BDNF* transgenic mice, the contralateral/ipsilateral (C/I) VEPs ratio was indistinguishable from that of the wild-type mice (Figure 7E; t test, $p = 0.31$; wild-type mice, $n = 4$; *BDNF* transgenic mice, $n = 3$).

To study ocular dominance plasticity, we measured the effects of 4 days of MD on C/I VEPs ratio recorded from binocular visual cortex contralateral to the deprived eye in wild-type and *BDNF* transgenic mice. The data shown in Figure 7D depict the effects of 4-day MD beginning at P28 (near the peak of ocular dominance plasticity; Gordon and Stryker, 1996) on the C/I VEPs ratio in a wild-type animal. The VEPs of the contralateral, deprived eye were greatly reduced in amplitude, while VEPs of the ipsilateral, nondeprived eye increased (Figures 7D and 7E), thereby shifting the C/I VEPs ratio to 1.2. This magnitude of reduction in contralateral bias, by 2.4-fold, was in the range of those reported by single-unit recordings (2.1-fold, Drager, 1975; 1.4- to 3.0-fold,

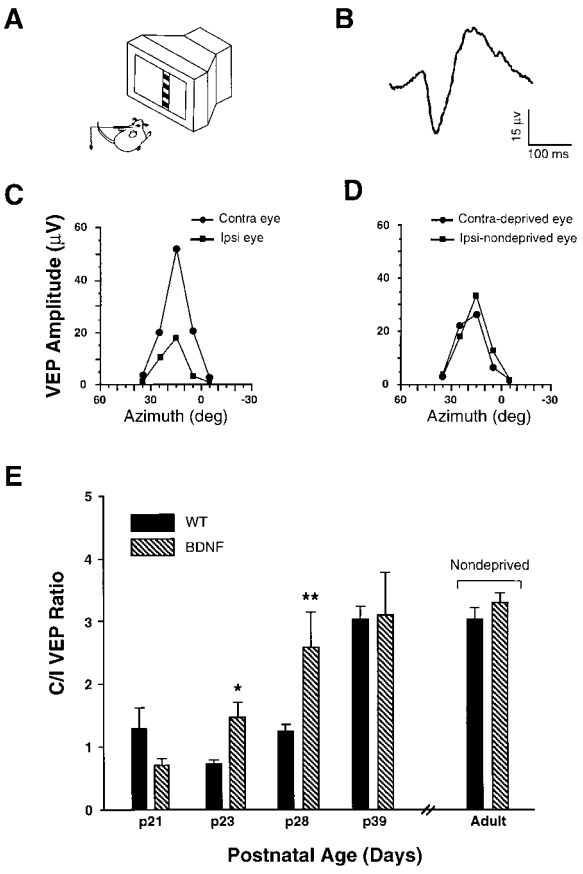

Figure 7. Precocious Termination of the Critical Period for Ocular Dominance Plasticity in *BDNF* Transgenic Mice

(A) Visual stimulus (a vertical stripe of 10° × 86° of a horizontal grating) was presented at different visual field azimuths to the anesthetized mice.

(B) Typical VEP waveform recorded from an electrode positioned in the binocular primary visual cortex, 400 μm below cortical surface. The response consists of a negative wave of a latency of 90–100 ms followed by a late positive wave. VEP amplitude was taken as peak-to-peak amplitude.

(C) For both the contralateral and ipsilateral eye, VEP amplitude is maximal when the stimulus is presented at an optimal azimuth. Note that responses of the contralateral eye are larger in amplitude than those of the ipsilateral eye.

(D) Effects of 4 days of monocular deprivation (MD) starting from P28 in wild-type mice. Note that the responses of the contralateral-deprived eye are reduced in amplitude, whereas those of the ipsilateral-open eye are increased.

(E) Effects of 4 days of MD starting at various ages on the contralateral/ipsilateral (C/I) VEP ratio in wild-type and *BDNF* mice. Note the different age dependence of the effect of MD in wild-type and *BDNF* mice. *BDNF* mice display an accelerated critical period for MD as compared to wild-type mice.

Gordon and Stryker, 1996). In contrast, MD beginning at P28 had little effect on C/I VEPs ratio in *BDNF* transgenic littermates (*BDNF* transgenics: C/I = 2.6 ± 0.49, $n = 4$; wild-type mice: C/I = 1.24 ± 0.12, $n = 6$; t test, $p < 0.001$; Figure 7E). A smaller but significant difference between *BDNF* transgenic and wild-type mice was also observed when 4-day MD started at P23 (*BDNF* transgenics: C/I = 1.48 ± 0.12, $n = 3$; wild-type mice: C/I = 0.72 ± 0.08, $n = 3$; t test, $p = 0.03$; Figure 7E).

When MD started at P21, *BDNF* transgenics tended to display a larger shift in C/I VEPs ratio compared with the wild-type mice, although the difference did not achieve a statistic significance (*BDNF* transgenics: C/I = 0.72 ± 0.09, n = 4; wild-type mice: C/I = 1.29 ± 0.32, n = 6; t test, p = 0.1). At P39, an age after the end of the critical period for ocular dominance shift in wild-type mice (Gordon and Stryker, 1996), MD had no effect on C/I VEPs ratio in either *BDNF* or wild-type mice (*BDNF* transgenics: C/I = 3.12 ± 0.66, n = 3; wild-type mice: C/I = 3.03 ± 0.21, n = 4; t test, p = 0.9).

Data obtained at all ages were submitted to a two-way ANOVA which revealed that the effect of MD depended on age ($F[3,32] = 16.9$, $p < 0.001$) and that this effect was different between *BDNF* transgenic mice and wild-type mice (interaction of age × mouse type: $F[3,32] = 4.03$, $p = 0.018$), indicating that the termination of ocular dominance plasticity was advanced in the transgenics. In other words, there was a precocious closure of the critical period of ocular dominance (OD) plasticity in the transgenic mice.

A Precocious Development of Visual Acuity in *BDNF* Transgenic Mice

We also measured the development of visual acuity in the *BDNF* transgenic mice using VEPs. VEP acuity is a well-established measure of overall visual function that can be used to predict the behavioral visual acuity in a number of mammals, including rats and mice (Birch, 1979; Gianfranceschi et al., 1999). Previous work has shown that there is a systematic increase in visual acuity during postnatal development (Freeman and Marg, 1975; Fagiolini et al., 1994).

As shown in Figures 8C and 8E, VEP acuity of wild-type mice was low (0.23 ± 0.02 cycle/deg; n = 4) at P20 and reached adult levels (0.57 ± 0.1 cycle/deg; n = 3) by P28–P31. In *BDNF* transgenic mice, the development of visual acuity was accelerated as compared to wild-type mice. At P20, visual acuity of *BDNF* transgenic mice was similar to their wild-type littermates (0.23 ± 0.03 cycle/deg; n = 4). In the next few days, however, the visual acuity of the transgenics greatly increased to reach adult levels by P24–P25, about 1 week earlier than those in wild-type mice. At this age, visual acuity of transgenics was higher than that of wild-type mice by nearly a factor of three (0.7 ± 0.08 cycle/deg; n = 4 versus 0.24 ± 0.02 cycle/deg, n = 4; Figures 8C and 8E). The mature visual acuity of *BDNF* and wild-type mice was comparable (0.7 ± 0.17 cycle/deg, n = 3 versus 0.6 ± 0.06 cycle/deg, n = 3; two-way ANOVA, effect of age: $F[3, 28] = 15.99$, $p < 0.001$; effect of genotype: $F[1, 28] = 11.39$, $p < 0.01$; interaction effect age × mouse type: $F[3, 28] = 4.97$, $p < 0.01$). Tukey's post hoc comparison showed that the only age at which *BDNF* and wild-type mice were significantly different was P24–P25 ($p < 0.01$).

The accelerated maturation of visual acuity in *BDNF* transgenic mice as compared to wild-type mice was not due to differences in optical factors, since in both mice the optical media were clear by P18. In addition, the contrast threshold, which is known to be strongly impaired by optical opacities (Campbell, 1965) was already adult-like at P20 both in *BDNF* transgenic and wild-type mice (Figures 8D and 8F; two-way ANOVA, effect of age: $F[4, 24] = 0.58$, $p = 0.68$; effect of genotype: $F[1, 24] = 0.53$, $p = 0.48$). These results indicate that the overexpression of a single neurotrophin BDNF leads to precocious development of visual acuity.

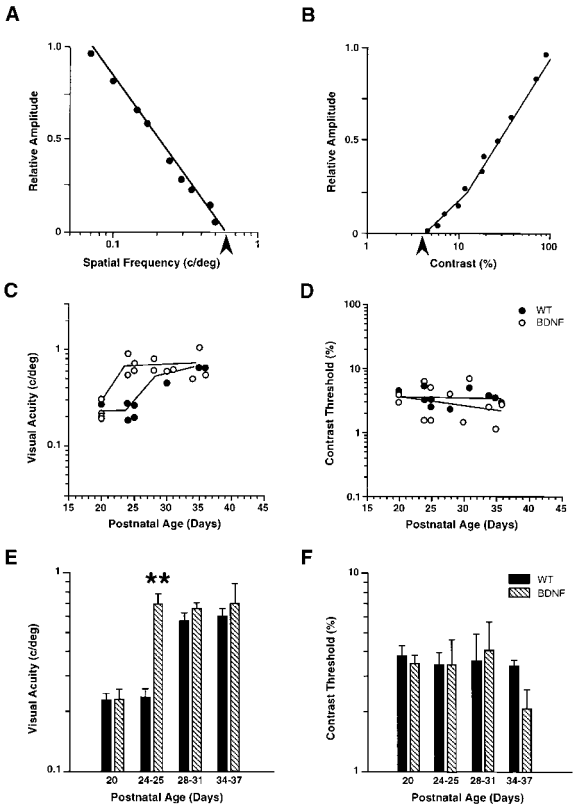

Figure 8. Precocious Development of Visual Acuity in *BDNF* Transgenic Mice

(A and B) VEP amplitude decreases with increasing stimulus spatial frequency (A) or decreasing contrast (B). Visual acuity and contrast threshold were determined by linearly extrapolating (solid line) to 0 V the set of data points recorded at the four highest resolvable (above the noise level) frequencies. Estimated values are indicated on the abscissae by a black arrow.

(C) Maturation of visual acuity is accelerated in *BDNF* transgenic mice. Visual acuity of single *BDNF* (open circles) and wild-type (filled circles) mice at different postnatal ages. Note that visual acuity of *BDNF* transgenic reaches adult levels already at P24–P25. At each age, same numbers of wild-type and *BDNF* mice were tested. Some data points of wild-type mice are not visible because they overlap with those of the transgenics. See text for numeric data.

(D) Contrast threshold is already adult-like at P20 both in *BDNF* transgenic and wild-type mice.

(E) Visual acuity from the same animals in (C) plotted as groups of age. Visual acuity of *BDNF* mice is significantly different from wild-type mice at P24–P25.

(F) Average contrast thresholds from the same animals in (D) do not show significant effects of age.

Discussion

BDNF Promotes the Postnatal Maturation of GABAergic Interneurons in the Visual Cortex

The postnatal maturation of GABAergic inhibitory neurons is a delayed and protracted process compared to

that of the excitatory neurons (reviewed in Micheva and Beaulieu, 1997). The amount and pattern of input neuronal activity have been shown to play key roles during the maturation of the inhibitory circuitry (e.g., Blue and Parnevelas 1983; Benevento et al., 1992, 1995; reviewed in Marty et al., 1997). Recently, BDNF was proposed to be a molecular signal that linked activity with changes of inhibition in neuronal culture (Rutherford et al., 1997). However, whether and how BDNF regulates the maturation of inhibition during the development of visual cortex have not been established. In our transgenic mice, the postnatal rise of BDNF in the visual cortex was genetically accelerated, but its cellular distribution was not substantially altered: BDNF overexpression was restricted to the pyramidal neurons in the visual cortex. Our data demonstrated that this developmentally accelerated BDNF expression also accelerated the maturation of GABAergic innervation and inhibition in the developing visual cortex. These results suggest that the maturation of the inhibitory circuitry impinges on the availability of BDNF in the third and forth postnatal week. During these postnatal weeks, endogenous BDNF levels in the visual cortex are still rising and are strongly influenced by visual experience such as dark rearing and monocular deprivation (Castren et al., 1992; Bozzi et al., 1995). Therefore, BDNF may play a key role in the normal maturation as well as in the activity-dependent plasticity of GABAergic interneurons during the critical period of visual cortical development.

The maturation of GAD65 puncta rings around the somata of pyramidal neurons may be due to either an increase in the level of this enzyme in the inhibitory presynaptic terminal or an increase in the number of inhibitory synaptic boutons, or both. In either case, the effects of BDNF overexpression on the maturation of GABAergic neurons are not cell autonomous, since the overexpression was restricted to pyramidal neurons. GABAergic neurons thus may have received the BDNF signal either from their postsynaptic (retrograde) or presynaptic (anterograde) pyramidal neurons. The presence of parvalbumin-positive boutons around BDNF-overexpressing somata (Figure 2C) is consistent with retrograde signaling. However, an anterograde effect of BDNF is also possible. For example, BDNF was shown to increase the quantal amplitudes of AMPA-mediated miniature excitatory postsynaptic currents from pyramidal neurons to GABAergic interneurons (Rutherford et al., 1998).

On the other hand, BDNF has also been implicated in regulating dendritic growth of cortical pyramidal neurons (e.g., McAllister et al., 1995). The development of the excitatory synaptic transmission in the visual cortex of *BDNF* transgenic mice remains to be analyzed in detail. However, our electrophysiological measurements so far did not reveal a difference in the strength of AMPA-mediated currents in layer III pyramidal neurons (Figure 5).

BDNF Overexpression Accelerates the Developmental Decline of WM-Evoked Layer III LTP

In an in vitro model of visual cortical plasticity, the developmental decline of WM-evoked, layer III LTP (WM→III LTP) closely parallels the decline of the susceptibility of binocular connections to effects of MD (Kato et al., 1991; Kirkwood et al., 1995; Perkins and Teyler, 1988). It was proposed that cortical inhibitory circuitry may contribute to a "plasticity gate" which limits the afferent activity patterns that can gain access to the modifiable synapses in layer III (Kirkwood and Bear, 1994). In *BDNF* transgenic mice, the maturation of the inhibitory circuitry as well as WM→III LTP was accelerated. Furthermore, LTP could be restored in slices from juvenile *BDNF* transgenic mice by application of a GABAA receptor antagonist. A parsimonious interpretation of these results is that BDNF overexpression reduces cortical plasticity early in postnatal life through the precocious development of the inhibitory circuitry. Thus, the "critical period" for synaptic plasticity in the superficial layer of the visual cortex may in part be determined by BDNF-mediated maturation of cortical inhibitory circuits.

The site of the inhibitory "plasticity gate" is believed to be within or deep to cortical layer IV, since direct high-frequency stimulation of layer IV reliably induces LTP in layer III regardless of age (Kirkwood and Bear, 1994). For technical reasons, our recordings of IPSCs were conducted in layer III instead of layer IV. However, the enhanced strength of inhibition in juvenile *BDNF* transgenic mice was well correlated with changes in GAD65 staining, which showed an accelerated maturation in both layer III and layer IV as compared to wild-type littermates. Thus, the precocious decline in WM→III LTP in the *BDNF* trangenic mice could be due to the earlier maturation of inhibition in layer IV, although we cannot exclude a role for the changes in layer III as well. In future studies, it will be of interest to investigate the laminar differences in inhibition in the *BDNF* transgenic mice.

BDNF Overexpression Results in Precocious Termination of the Critical Period of Ocular Dominance Shift

Neurotrophins have been hypothesized to function as substrates for activity-dependent synaptic competition in the developing visual system (Maffei et al., 1992; Thoenen, 1995). In such a model, neurotrophins are present in a limited amount in postsynaptic neurons and act rapidly and locally to strengthen active presynaptic inputs. Less active and/or less correlated presynaptic inputs then lose out in the competition for neurotrophins (Figure 9A). Consistent with this idea, intracortical infusion of trkB ligands was shown to disrupt the formation of ocular dominance columns in cats (Cabelli et al., 1995) and rescue LGN neurons from the effect of MD in ferrets (Riddle et al., 1995). In rodents, intraventricular infusion of NGF during the critical period prevented the ocular dominance shift in favor of the nondeprived eye (Maffei et al., 1992; Carmignoto et al., 1993).

In most of these pharmacological experiments, high concentrations of neurotrophins were applied extracellularly and therefore bypassed the cellular regulation of neurotrophin release (Blochl and Thoenen, 1995). In our transgenic mice, the excess BDNF protein is produced within pyramidal neurons that normally express BDNF, and thus it is likely to be processed and released as the endogenous BDNF. In these BDNF overexpressing mice, the ocular dominance plasticity was indeed

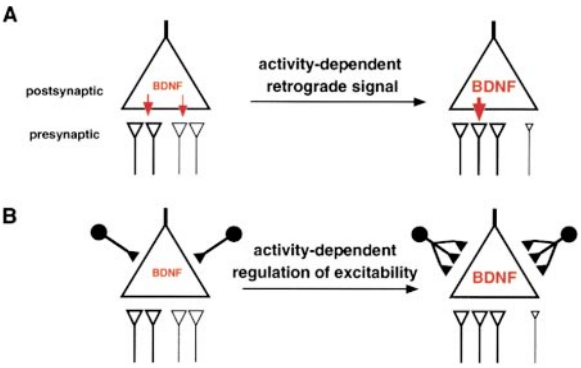

Figure 9. Two Models on Different Aspects of BDNF Function in Synaptic Plasticity

Large open triangles, excitatory postsynaptic neurons; small open triangles, excitatory presynaptic inputs; black circles and triangles, inhibitory neurons and synapses.

(A) BDNF as an activity-dependent retrograde signal at excitatory synapses. BDNF is present in limited amount in the postsynaptic neuron and is released in an activity-dependent manner (red arrows). They then act rapidly and locally to strengthen active presynaptic inputs, which are correlated with activity of the postsynaptic neuron (bold, small triangles). Less active and/or less correlated presynaptic input then lose out in the competition for limited amount of neurotrophins (plain small and smallest triangles).

(B) BDNF mediates activity-dependent regulation of plasticity threshold. The amount of BDNF in a cortical pyramidal neuron (represented by the size of "BDNF" in red) is proportional to the level of its chronic firing activity. BDNF-regulated inhibition, which may occur in the time scale of many hours or even days, alters the amount of postsynaptic depolarization produced by excitatory inputs and, therefore, the firing threshold of the neuron. Thus, in chronically active neurons, BDNF levels would be high and inhibition would be strong; as a consequence, only strong and/or correlated inputs could continue to drive the postsynaptic neurons and prevail (bold, small triangles). Weaker and/or less correlated inputs become increasingly subthreshold and are destined for elimination (plain small and smallest triangles). See text for details.

blocked when MD was performed at P28 (Figure 7E), near the peak of OD shift in wild-type mice (Gordon and Stryker, 1996). However, at P21 when BDNF overexpression was substantial (much higher than that in P35 wild-type mice, Figure 1D), MD did produce normal OD shift with a magnitude similar to, if not larger than, that in wild-type littermates (Figure 7E). Consistent with our VEP findings, single-unit recording experiments have yielded similar results and have shown that OD plasticity was even enhanced in the transgenic mice at P21 (Hanover et al., unpublished data). Taken together, these results indicate that BDNF overexpression does not block OD plasticity, but rather results in a precocious closure or even an early shift of the critical period of plasticity. These findings further suggest that simple competition for BDNF cannot be the only mechanism for OD plasticity.

Since the precocious closure of the critical period for OD plasticity in the transgenic mice correlated with the accelerated maturation of GABAergic circuitry and earlier developmental decline of WM→III LTP, we propose that BDNF may play a key role in ocular dominance plasticity and its critical period in part through regulating the maturation of GABAergic inhibition. The maturation of inhibition could have two apparently opposite consequences. First, the development of an appropriate level of inhibition may be necessary for ocular dominance plasticity, as suggested by the fact that the peak of OD shift does not occur until the fourth postnatal week in normal animals (Gordon and Stryker, 1996). This notion was supported by the finding that OD plasticity was abolished in *GAD65* knockout mice and was restored by pharmacological enhancement of GABAergic transmission (Hensch et al., 1998). Also consistent with this notion was our data (Figure 7), suggesting that the developmental kinetics of OD shift were advanced by several days in the *BDNF* transgenic mice

Second, the full maturation of the cortical inhibitory circuitry may constrain the activation of cortical synapses, thereby reducing plasticity that would otherwise be induced by the imbalance of visual input during MD. Consistent with this notion, the accelerated maturation of GABAergic inhibition in *BDNF* transgenic mice correlated with, and may also have contributed to, the earlier closure of the critical period. Conversely, dark rearing has been shown to retard the maturation of visual cortical GABAergic circuitry (Benevento et al., 1992, 1995) and prolong critical periods for both WM→III LTP (Kirkwood et al., 1995) and ocular dominance plasticity (Fagiolini et al., 1994). The effects of dark rearing on inhibitory circuitry may in part be mediated by the downregulation of BDNF expression in the visual cortex (Castren et al., 1992). To our knowledge, there has previously been no genetic manipulation that altered the timing of a critical period for the development of a sensory cortex.

At present we cannot rule out the possibility that other processes such as NMDA receptor mechanisms (Carmignoto and Vicini, 1992; Sheng et al., 1994) were also affected by the *BDNF* transgene. An earlier decline of NMDA receptor function in layer IV of the visual cortex could contribute to the reduction of OD plasticity and therefore an earlier closure of the critical period, as well as a precocious decline of WM→III LTP. The *BDNF* transgenic mice provide a model system to investigate these additional cellular mechanisms involved in the regulation of critical period.

BDNF Accelerates the Development of Visual Acuity

In all mammals tested so far, there is an experience-dependent increase in visual acuity during postnatal development (Freeman and Marg, 1975; Boothe, 1985; Fagiolini et al., 1994). In *BDNF* transgenic mice, adult level of visual acuity was reached about a week earlier than that in wild-type littermates. Interestingly, the increase of visual acuity is well correlated with a decrease of mean receptive field size of neurons in the primary visual cortex (Fagiolini et al., 1994). The role of cortical inhibition in the generation of neuronal receptive field properties is suggested by experiments showing that extracellular application of GABA antagonist in the somatosensory or visual cortex profoundly alters these properties (Sillito, 1979; Hicks and Dykes, 1983). The precocious increase of visual acuity in *BDNF* transgenic mice therefore might be causally linked to the accelerated development of cortical inhibition. However, BDNF overexpression might also affect the development of the excitatory synaptic transmission and as a result contribute to the increase of visual acuity. Regardless of

the mechanism, our results suggest that BDNF overexpression is sufficient to accelerate the development of visual acuity. There have been no pharmacological or genetic manipulations that could dramatically accelerate the development of visual function.

BDNF and Synaptic Plasticity

Current thinking on the role of neurotrophins in synaptic plasticity has focused mainly on excitatory neurons and synapses. However, ocular dominance plasticity is also profoundly influenced by manipulation of inhibitory mechanisms (Reiter and Stryker, 1988; Hata and Stryker, 1994). The formation and maintenance of inhibitory synapses in the developing CNS are regulated by neuronal activity (reviewed in Marty et al., 1997; Micheva and Beaulieu, 1997). Our results, together with recent studies in neuronal culture (Rutherford et al., 1997, 1998), suggest that BDNF may mediate developmental and activity-dependent regulation of GABAergic inhibition, which in turn could modify the firing threshold of the excitatory neurons.

Consider a model in which the amount of BDNF in a cortical pyramidal neuron is proportional to the level of its chronic firing activity (Figure 9B). Because BDNF is involved in regulating the number and/or efficacy of inhibitory synapses, the amount of inhibition that a pyramidal cell receives thus reflects its activation history (Figure 9B). Previous theoretical work suggested the existence of a critical level of postsynaptic depolarization that determines the direction of synaptic modification (i.e., strengthening or weakening) and changes as a function of the history of the integrated postsynaptic activity (Bienenstock et al., 1982; Bear et al., 1987). Activity-dependent and BDNF-mediated regulation of GABAergic inhibition could, in principle, provide a cellular basis for such a sliding synaptic modification threshold. Thus, during the critical period, in chronically active pyramidal neurons, BDNF levels would be high and inhibition would be strong; as a consequence, only the strong and most highly correlated inputs would satisfy the conditions for synaptic potentiation. Weak and poorly correlated inputs (e.g., those from the deprived eye during MD) would become subthreshold and be depressed and eliminated. On the other hand, if activity levels are low (as in dark rearing), BDNF levels and the strength of inhibition would fall. The consequence of these changes would be to lower the synaptic modification threshold such that weaker or less correlated inputs could also satisfy the conditions required for synaptic strengthening.

This "plasticity threshold" model does not incorporate a very rapid and local mode of BDNF action. By altering the amount of postsynaptic depolarization, which influences voltage-dependent ion channels including NMDA receptors, BDNF-regulated inhibition could modify the known correlation-based plasticity mechanisms, such as LTP and long-term depression (LTD). It should be emphasized that the "plasticity threshold" model of BDNF function does not contradict the "retrograde messenger" model. They are likely to represent different aspects of BDNF functions at different subcellular compartments and different time scales. Cell type–restricted manipulation (e.g., pyramidal neurons versus GABAergic interneurons) of the trkB/BDNF receptors may be necessary in further understanding how the acute effect of BDNF on excitatory synapses (Akaneya et al., 1997; Huber et al., 1998) and the chronic effects of BDNF on inhibitory synapses fit together in regulating cortical plasticity.

Experimental Procedures

Generation of Transgenic Mice and Genotyping

A Kozac sequence was inserted in front of the translation initiation site of the rat *BDNF* cDNA by recombinant PCR. This DNA fragment was then cloned into the XhoI site of pMSG (Pharmacia) to generate pJH101, in which the SV40 intron/poly(A) was at the 3′ end of the *BDNF* cDNA. The 1.6 kb SalI and BamHI fragment of pJH101 (including the *BDNF* cDNA and SV40 intron/poly[A]) was then blunt-end ligated into the NotI site of pNN279 containing the 8.5 kb CaMKIIα promoter (pJH102). The 10.1 kb SalI fragment of pJH102 containing the CaMKIIα promoter and the *BDNF* transgene was purified. Transgenic mice were generated by microinjection of linearized transgene into the BDF2 hybrid embryos. Founders were backcrossed into C57BL6 background. Mice were screened for the transgene by PCR and Southern blotting for routine genotyping.

Northern Blot

Mice were sacrificed by cervical dislocation. Various parts of the brain were quickly dissected in ice-cold PBS and frozen immediately in liquid nitrogen. Total RNA was isolated using the TRI reagent kit (Molecular Research Center, Inc.). Approximately 20 μg of total RNA was used for Northern analysis following standard procedures (Sambrook et al. 1989). The blot was hybridized with DNA probes containing, respectively, the *BDNF* cDNA, SV40 poly(A) (pMSG, Pharmacia), or human G3PDH (Clontech). Quantification was done with a Fujix Bioimaging Analyzer based on data from two experiments. Total *BDNF* mRNA was calculated by adding the intensity of relevant bands (1.6 kb and 4.0 kb endogenous and 1.6 kb transgenic) and then normalized according to the G3PDH signal. G3PDH signal of P35 WT (Figure 1D) was used as standard.

In Situ Hybridization

Mice were killed, and the brains were dissected and rapidly frozen in mounting medium. Cryostat sections (20 μm) were taken, postfixed for 10 mm in 4% paraformaldehyde in PBS (pH 7.3), dehydrated, and stored frozen at −70°C until use. The slices were hybridized to a *BDNF* oligonucleotide probe (5′-CAGTTGGCCTTTTGATAC CGGGACTTTCTCCAGGACTGTGACCGTCCC-3′), which detects both the endogenous and the transgenic *BDNF* mRNA, or a SV40 oligonucleotide probe (5′ GTCACACCACAGAAGTAAGGTTCCTTCA CAAAGATCCCTCGAGATGC-3′) specific for the transgenic *BDNF* mRNA (data not shown). The probes were labeled by 3′ poly(A) tailing using [α-^{35}S]thio-dATP and terminal transferase to a specific activity of 0.5×10^8 to 1×10^8 cpm/μg. Hybridization was overnight at 42°C in a solution containing 50% formamide, 10% dextran sulfate, 25 mM HEPES (pH 7.0), 600 mM NaCl, 100 mM DTT, 1× Denhardt's, 200 μg/ml denatured salmon sperm DNA, 200 μg/ml poly(dA), and 10^7 cpm/ml oligonucleotide probe. Slides were washed two times for 10 min each in 2× SSC at room temperature and two times for 60 min each in 0.2× SSC at 65°C, dried, and exposed to film for 2 weeks.

Immunohistochemistry

Mice were anesthetized and perfused intracardially with cold saline (0.9% NaCl) followed by freshly prepared 4% paraformaldehyde in 0.1 M phosphate buffer (pH 7.4). Brains were postfixed in the same solution for less than 2 hr at 4°C and were equilibrated first in 15% sucrose and then 30% sucrose in PBS overnight. They were then cut into 20 μm coronal sections in a cryostat (Leica) and stored at −80°C. For immunohistochemistry (IHC) experiments, sections from wild-type and transgenic animals were always reacted simultaneously. Quantification and comparison were made among samples

from the same experiment. Since BDNF overexpression was restricted to the forebrain in the transgenics, the variability in immunostaining was controlled by selecting wild-type and transgenic samples in which the staining intensities were similar in brain areas other than the cerebral cortex and hippocampus. One adult *BDNF* transgenic mouse and one wild-type littermate were used for BDNF IHC. Briefly, an affinity-purified anti-BDNF antiserum (a kind gift from Dr. Qiao Yan, Amgen Co.) was used at 0.1 μg/ml, a concentration 5-fold less than suggested in Yan et al. (1997). The secondary biotinylated goat anti-rabbit antibody was used at 2 μg/ml and detected with the avidin-biotin-peroxidase complex method (Vector Labs). For parvalbumin IHC, brain samples from the following ages were used: P12 (two *BDNF* transgenic, two wild-type littermates), P17 (three *BDNF* transgenic, three wild-type littermates), P24 (three *BDNF* transgenic, three wild-type littermates), and P35 (three *BDNF* transgenic, three wild-type littermates). A monoclonal antibody against parvalbumin (Sigma) was used at 1:5000 dilution in 10% normal horse serum (NHS), 0.2% Triton in PBS. The secondary biotinylated horse anti-mouse antibody was used at 2 μg/ml and detected with the avidin-biotin-peroxidase complex method (Vector Labs). To quantitate the density of parvalbumin neurons in the visual cortex, parvalbumin immunoreactive neurons within two 500 μm × 500 μm areas in each hemisphere of the visual cortex were counted under light microscope, using a 20× objective. At least six coronal sections from each genotype at each age were analyzed. Data from the same genotype at the same age were pooled and averaged. A single-factor ANOVA was applied to determine whether the difference between *BDNF* transgenic and wild-type littermates at each age was statistically significant. For GAD65 IHC, the same groups of animals were used as for parvalbumin IHC. In addition, three *BDNF* transgenic and three wild-type littermates at P21 were included. A monoclonal antibody (GAD-6, Boehringer Mannheim) was used at a dilution of 1:500 in 1% NHS, 0.2% Triton in PBS. The secondary fluorescein anti-mouse IgG (Vector) was used at 1:200 dilution in the same buffer as for the primary antibody. The GAD65 immunostaining was analyzed using confocal laser scanning microscopy (CLSM) as detailed below.

Confocal Laser Scanning Microscopy

GAD65 monoclonal antibody labeled brain sections were first examined under epifluorescense microscope at 20× and 40× objectives to locate layers 2, 3, and 4 of the visual cortex. GAD65 immunoreactive terminals and synaptic boutons were then examined under a 100× oil immersion objective using a confocal laser scanning microscope (BioRad MRC-1024ES). At least six coronal sections from 2–3 animals from each genotype at each age were analyzed. Images were acquired using laser excitation wavelength at 488 nm and emission filter 522DF35. Laser power was kept at 3% and aperture (or iris) size kept at 3.0. Each image was scanned and averaged ten times, saved as TIFF files, and analyzed with NIH Image software. For each image, perisomatic GAD65 signals (puncta ring) from five target neurons were outlined and signal density quantified (pixel value/μm^2) and averaged; in addition, GAD65 signals in five areas (each approximately 200–400 μm^2 in size) in the neuropil region were quantified and averaged (N); finally, the cell soma of five neurons (which should be devoid of GAD65 signal) were selected, and the signal density was averaged as background (B). The average intensity of GAD65 in puncta rings in this image was then calculated as (P − B). The average intensity of GAD65 in neuropil in this image was calculated as (N − B). Data from at least eight images from the same genotype at each age were then averaged to derive the value of GAD65 "puncta" and GAD65 "neuropil" shown as pixel value/μm^2 in Figure 4B. A single-factor ANOVA was applied to determine whether the difference between *BDNF* transgenic and wild-type littermates at each age was statistically significant.

For double labeling, BDNF antibody (Qiao Yan et al., 1997) was used at 0.1 μg/ml and visualized with Alexa 488 (Molecular Probe, 1:200 dilution). Monoclonal antibodies against parvalbumin (Sigma) and CaMKIIα (GIBCO) were used at 1:2000 and 1:200, respectively, and were visualized with Alexa 594 (Molecular Probe, 1:200 dilution). Labeled tissues were examined under a 63× water immersion objective (Zeiss, NA = 1.2). Laser excitation wavelengths and emission filter were 488 nm and 522DF35 for Alexa 488, and 568 nm and HQ598DF40 for Alexa 594. Five to seven images were acquired in the double labeling mode at 1.0 μm interval in a z-series. The detection aperture was kept the same for the two channels. Images from each channel were collected in sequential series mode and were subsequently merged. Care was taken to use the lowest laser power, and no bleed through was visible between the Alexa 488 to the Alexa 594 channels even in nonsequential mode. To produce a 3D reconstruction of the z-series, the optical sections from each scanned and merged image were projected and compiled into a single image. They were saved as TIFF files and processed in Adobe Photoshop 5.0.

Electrophysiology in Visual Cortical Slice

Brain slices from visual cortex were prepared as described previously (Kirkwood et al., 1997). The slices were maintained in an interface storage chamber containing artificial cerebrospinal fluid (ACSF) at 30°C for at least 1 hr prior to recording. The ACSF was saturated with 95% O_2 and 5% CO_2 and contained, in mM, NaCl: 124, KCl: 5, NaH_2PO_4: 1.25, $MgCl_2$: 1, $CaCl_2$: 2, $NaHCO_3$: 26, dextrose: 10. Voltage clamp measurements were performed on submerged slices, continuously perfused at a rate of 2 ml/min with 30°C ASCF saturated with 95% O_2 and 5% CO_2. In all other experiments, the slices were kept in an interface chamber with an atmosphere of humidified 95% O_2 and 5% CO_2 and superfused with 30°C ACSF at a rate of 1 ml/min. Stimulation was applied either at the white matter–layer VI border (WM stimulation) or at site in the middle of the cortical thickness, confirmed histologically to correspond to layer IV and upper layer V. Whole-cell patch–clamp recordings were made from layer II/III pyramidal neurons visualized by IR-DIC videomicroscopy (Zeiss Axioscope) using a Warner PC-505A amplifier (Warner instrument Corporation). Patch electrodes (2–6 MΩ) were filled with internal solution (in mM): 130 cesium gluconate, 2 $MgCl_2$, 2 $CaCl_2$, 10 EGTA, 10 HEPES, 2 Na-ATP, 10 QX-314; pH was adjusted to 7.25 with CsOH; 275–285 mOsm. For analysis, we considered only those cases in which the initial access resistance was less than 15 MΩ and the input resistance was larger than 250 MΩ. Data were discarded if during the experiment the access resistance increased to a value >20 M9Ω or if the cell's input resistance decreased below 100 MΩ. The reversal potential of the IPSC was determined in the presence on 10 μM CNQX and 100 μM APV to block AMPA and NMDA receptor–mediated responses. Likewise, the reversal potential of the EPSC was determined in the presence of 10 mM biccuculine methiodide (BMI) to reduce GABAA responses.

The extracellular field potential responses (FP) were recorded as previously described (Kirkwood and Bear 1994). Only data from slices with stable recordings (<5% change over the baseline period) were included in the analysis and analyzed as follows: (1) the maximum negative FP amplitude data for each experiment were expressed as percentages of the preconditioning baseline average, (2) the time scale in each experiment was converted to time from the onset of conditioning, and (3) the time-matched, normalized data were averaged across experiments and expressed as the means (± SEM). Within each group, the statistical significance of a change produced by conditioning stimulation was assessed with a paired t test, comparing values immediately before conditioning stimulation with those 30 min after TBS. Mutant and wild-type groups of different ages were compared at the time point 30 min after TBS using a two-way ANOVA. Cumulative histograms were also constructed to show the data from each slice in each group.

VEP Recordings

The technique of VEP recording in mice has been previously described (Porciatti et al., 1999). All measurements were performed in the primary binocular visual cortex 10°–20° from the vertical meridian in anesthetized mice. Briefly, a large portion of the skull (4 mm × 4 mm) overlying the visual cortex was carefully drilled and removed leaving the dura intact. A resin-coated microlectrode (WPI, Sarasota) with tip impedance of 0.5 MΩ was inserted into the cortex perpendicularly to the stereotaxic plane. Microelectrodes were inserted 2.6–3.2 mm lateral to the lambda, and advanced 400 μm within the cortex. At this depth, VEPs had their maximal amplitude. The region of the visual field yielding VEPs of maximal amplitude (VEP receptive field azimuth) was established for each penetration by recording a

series of responses to stimuli windowed to a vertical stripe of 10° × 86° and presented at several different visual field azimuths (Porciatti et al., 1999; Figures 7A and 7C). The cortical representation of the vertical meridian was then established.

Electrical signals were amplified (50,000-fold), band–pass filtered (0.3–100 Hz, −6 dB/oct), digitized (12 bit resolution), and averaged (at least 128 events in blocks of 16 events each) in synchrony with the stimulus contrast reversal. Transient VEPs in response to abrupt contrast reversal (1 Hz) were evaluated in the time domain by measuring the peak-to-trough amplitude and peak latency of the major negative component (see example in Figure 7B). Visual stimuli were horizontal sinusoidal gratings of different spatial frequency and contrast generated by a VSG2/2 card (Cambridge Research System, Cheshire, UK) by custom software and presented on the face of TV display (Barco CCID 7751, Belgium) suitably linearized by gamma correction.

To assess the time course of the critical period for monocular deprivation, mice of various ages (P20–21, P23, P28–29, P39–40) were anesthetized with avertin (tribromoethanol in amylene hydrate, 20 μl/g of body weight administered intraperitoneally). Lid margins were trimmed and sutured with 7-0 silk. Mice were allowed to recover from anesthesia and were returned to their cages. The effectiveness of lid closure was checked daily. Mice showing occasional lid reopening were not included in the experiments. Four to five days after eyelids suture, the effects of monocular deprivation were assessed using VEPs. Immediately before the recording session the lids were cut, and the eye washed with saline and carefully inspected to verify that the surgical procedure did not cause any damage. The relative contribution of the two eyes to cortical responses was defined as the amplitude ratio between the responses to stimulation of the contralateral eye and that of the ipsilateral eye with stimuli of low spatial frequency. The contralateral to ipsilateral amplitude ratio was evaluated by integrating responses to stimuli presented at different azimuths (10° steps).

Acknowledgments

We thank Qiao Yan (Amgen Co.) for the BDNF antibody, Wenjiang Yu and Lydia J. F. Nelson for excellent technical assistance, Shona Chattarji for advice on the confocal microscopy, and Matthew Anderson and Pato Hureta for critical reading of the manuscript. Z. J. H. was a postdoctoral fellow of the Damon-Runyon Walter-Winchell Foundation. S. T and M. B. are investigators of HHMI. This work was supported by National Institutes of Health grant NS32925 and gifts from the Shonogi Institute for Medical Science to S. T.; L. M. acknowledges the support of EEC contract BMH4-CT96-1604, CNR target project on biotechnology (Linea 5.3.1), and CNR Italy/USA bilateral project. A. K acknowledges the support of National Eye Institute grant RO1EY12124-01 and the Sloane Foundation.

Received September 24, 1998; revised August 18, 1999.

References

Akaneya, Y., Tsumoto, T., Kinoshita, S., and Hatanaka, H. (1997). Brain-derived neurotrophic factor enhances long-term potentiation in rat visual cortex. J. Neurosci. *17*, 6707–6716.

Artola, A., and Singer, W. (1987). Long-term potentiation and NMDA receptors in rat visual cortex. Nature *330*, 649–652.

Bear, M.F., Cooper, L.N., and Ebner, F. (1987). A physiological basis for a theory of synapse modification. Science *237*, 42–48.

Benevento, L.A., Bakkum, B.W., Port, J.D., and Cohen, R.S. (1992). The effects of dark-rearing on the electrophysiology of the rat visual cortex. Brain Res. *572*, 198–207.

Benevento, L.A., Bakkum, B.W., and Cohen, R.S. (1995). gamma-aminobutyric acid and somatostatin immunoreactivity in the visual cortex of normal and dark-reared rats. Brain Res. *689*, 172–182.

Bienenstock, E.L., Cooper, L.N., and Munro, P.W. (1982). Theory for the development of neuron selectivity: orientation specificity and binocular interaction in visual cortex. J. Neurosci. *2*, 32–48.

Birch, D.J.G. (1979). Spatial contrast sensitivity in albino and pigmented rats. Vision Res. *19*, 933–937.

Blochl, A., and Thoenen, H. (1995). Characterization of nerve growth factor (NGF) release from hippocampal neurons: evidence for a constitutive and an unconventional sodium-dependent regulated pathway. Eur. J. Neurosci. *7*, 1220–1228.

Blue, M.E., and Parnevelas, P.J. (1983). The formation and maturation of synapses in the visual cortex of the rat. II. Quantitative analysis. J. Neurocytol. *12*, 697–712.

Bonhoeffer, T. (1996). Neurotrophins and activity-dependent development of the neocortex. Curr. Opin. Neurobiol. *6*, 119–126.

Boothe R.G., Dobson, V., and Telle, D.Y. (1985). Postantal development of vision in humans and in non human primates. Annu. Rev. Neurosci. *8*, 495–545.

Bozzi, Y., Pizzorusso, T., Cremisi, F., Rossi, F.M., Barsacchi, G., and Maffei, L. (1995). Monocular deprivation decreases the expression of messenger RNA for brain-derived neurotrophic factor in the rat visual cortex. Neuroscience *69*, 1133–1144.

Burgin, K.E., Waxham, M.N., Rickling, S., Westgate, S.A., Mobley, W.C., and Kelly, P.T. (1990). In situ hybridization histochemistry of Ca2+/calmodulin-dependent protein kinase in developing rat brain. J. Neurosci. *10*, 1788–1798.

Cabelli, R.J., Hohn, A., and Shatz, C.J. (1995). Inhibition of ocular dominance column formation by infusion of NT-4/5 or BDNF. Science *267*, 1662–1666.

Cabelli, R.J., Shelton, D.L., Segal, R.A., and Shatz, C.J. (1997). Blockade of endogenous ligands of trkB inhibits formation of ocular dominance columns. Neuron *19*, 63–76.

Campbell F.W., and Green, D.C. (1965). Optical and retinal factors affecting visual resolution. J. Physiol. (Lond.) *181*, 576.

Carmignoto, G., and Vicini, S. (1992). Activity-dependent decrease in NMDA receptor responses during development of the visual cortex. Science *258*, 1007–1011.

Carmignoto, G., Canella, R., Candeo, P., Comelli, M.C., and Maffei, L. (1993). Effects of nerve growth factor on neuronal plasticity of the kitten visual cortex. J. Physiol. (Lond.) *464*, 343–360.

Castren, E., Zafra, F., Thoenen, H., and Lindholm, D. (1992). Light regulates expression of brain-derived neurotrophic factor mRNA in rat visual cortex. Proc. Natl. Acad. Sci. USA *89*, 9444–9448.

Cellerino, A., Maffei, L., and Domenici, L. (1996). The distribution of brain-derived neurotrophic factor and its receptor trkB in parvalbumin-containing neurons of the rat visual cortex. Eur. J. Neurosci. *8*, 1190–1197.

Cohen, C.S., and Fraser, S.E. (1995). Effects of brain-derived neurotrophic factor on optic axon branching and remodelling in vivo. Nature *378*, 192–196.

Cohen, C.S., Dreyfus, C.F., and Black, I.B. (1991). NGF and excitatory neurotransmitters regulate survival and morphogenesis of cultured cerebellar Purkinje cells. J. Neurosci. *11*, 462–471.

Collazo, D., Takahashi, H., and McKay, R.D. (1992). Cellular targets and trophic functions of neurotrophin-3 in the developing rat hippocampus. Neuron *9*, 643–655.

Cynader, M., and Mitchell, D.E. (1980). Prolonged sensitivity to monocular deprivation in dark-reared cats. J. Neurophysiol. *43*, 1026–1040.

Del Rio, J.A., de Lecea, L., Ferrer, I., and Soriano, E. (1994). The development of parvalbumin-immunoreactivity in the neocortex of the mouse. Brain Res. Dev. Brain Res. *81*, 247–259.

Del Rio, J.A., Soriano, E., and Ferrer, I. (1992). Development of GABA-immunoreactivity in the neocortex of the mouse. J. Comp. Neurol. *326*, 501–526.

Diamond, J., Holmes, M., and Coughlin, M. (1992). Endogenous NGF and nerve impulses regulate the collateral sprouting of sensory axons in the skin of the adult rat. J. Neurosci. *12*, 1454–1466.

Drager, U. (1975). Receptive fields of single cells and topography in mouse visual cortex. J. Comp. Neurol. *160*, 269–290.

Drager, U., and Olsen, J. (1980). Origins of crossed and uncrossed retinal projections in pigmented and albino mice. J. Comp. Neurol. *191*, 383–412.

Dupuy, S.T., and Houser, C.R. (1996). Prominent expression of two forms of glutamate decarboxylase in the embryonic and early postnatal rat hippocampal formation. J. Neurosci. *16*, 6919–6932.

Ernfors, P., Lee, K.F., and Jaenisch, R. (1994). Mice lacking brain-derived neurotrophic factor develop with sensory deficits. Nature *368*, 147–150.

Esclapez, M., Tillakaratne, N.J., Kaufman, D.L., Tobin, A.J., and Houser, C.R. (1994). Comparative localization of two forms of glutamic acid decarboxylase and their mRNAs in rat brain supports the concept of functional differences between the forms. J. Neurosci. *14*, 1834–1855.

Fagiolini, M., Pizzorusso, T., Berardi, N., Domenici, L., and Maffei, L. (1994). Functional postnatal development of the rat primary visual cortex and the role of visual experience: dark rearing and monocular deprivation. Vision Res. *34*, 709–720.

Figurov, A., Pozzo, M.L., Olafsson, P., Wang, T., and Lu, B. (1996). Regulation of synaptic responses to high-frequency stimulation and LTP by neurotrophins in the hippocampus. Nature *381*, 706–709.

Freeman, D.N., and Marg, E. (1975). Visual acuity development coincides with the sensitive period in kittens. Nature *254*, 614–615.

Galuske, R.A., Kim, D.S., Castren, E., Thoenen, H., and Singer, W. (1996). Brain-derived neurotrophic factor reversed experience-dependent synaptic modifications in kitten visual cortex. Eur. J. Neurosci. *8*, 1554–1559.

Ghosh, A., and Greenberg, M.E. (1995). Distinct roles for bFGF and NT-3 in the regulation of cortical neurogenesis. Neuron *15*, 89–103.

Gianfranceschi, L., Fiorentini, A., and Maffei, L., (1999). Behavioral visual acuity of the wild-type and bcl-2 mouse. Vision Res. *39*, 569–574.

Gonchar, Y., and Burkhalter, A. (1997). Three distinct families of GABAergic neurons in rat visual cortex. Cereb. Cortex *7*, 347–358.

Goodman, C.S., and Shatz, C.J. (1993). Developmental mechanisms that generate precise patterns of neuronal connectivity. Cell *72*, 77–98.

Gorba, T., and Wahle, P. (1999). Expression of TrkB and TrkC but not BDNF mRNA in neurochemically identified interneurons in rat visual cortex in vivo and in organotypic cultures. Eur. J. Neurosci. *11*, 1179–1190.

Gordon, J.A., and Stryker, M.P. (1996). Experience-dependent plasticity of binocular responses in the primary visual cortex of the mouse. J. Neurosci. *16*, 3274–3286.

Hata, Y., and Stryker, M.P. (1994). Control of thalamocortical afferent rearrangement by postsynaptic activity in developing visual cortex. Science *265*, 1732–1735.

Hensch, T., Fagiolini M., Mataga N., Stryker, M.P., Baekkeskov, S, and Kash, S.F. (1998). Local GABA circuit control of experience-dependent plasticity in developing visual cortex. Science *282*, 1504–1508.

Hicks, T.P., and Dykes, R.W. (1983). Receptive field size for certain neurons in primary somatosensory cortex is determined by GABA-mediated intracortical inhibition. Brain Res. *274*, 160–164.

Huber, K.M., Sawtell, N.B., and Bear, M.F. (1998). Brain-derived neurotrophic factor alters the synaptic modification threshold in visual cortex. Neuropharmacology *37*, 571–579.

Ip, N.Y., Li, Y., Yancopoulos, G.D., and Lindsay, R.M. (1993). Cultured hippocampal neurons show responses to BDNF, NT-3, and NT-4, but not NGF. J. Neurosci. *13*, 3394–3405.

Isackson, P.J., Huntsman, M.M., Murray, K.D., and Gall, C.M. (1991). BDNF mRNA expression is increased in adult rat forebrain after limbic seizures: temporal patterns of induction distinct from NGF. Neuron *6*, 937–948.

Jones, K.R., Farinas, I., Backus, C., and Reichardt, L.F. (1994). Targeted disruption of the BDNF gene perturbs brain and sensory neuron development but not motor neuron development. Cell *76*, 989–999.

Kang, H., and Schuman, E.M. (1995). Long-lasting neurotrophin-induced enhancement of synaptic transmission in the adult hippocampus. Science *267*, 1658–1662.

Kato, N., Artola, A., and Singer, W. (1991). Developmental changes in the susceptibility to long-term potentiation of neurons in rat visual cortex slices. Brain Res. Dev. Brain Res. *60*, 43–50.

Katz, L.C., and Shatz, C.J. (1996). Synaptic activity and the construction of cortical circuits. Science *274*, 1133–1138.

Kirkwood, A., and Bear, M.F. (1994). Hebbian synapses in visual cortex. J. Neurosci. *14*, 1634–1645.

Kirkwood, A., Lee, H.K., and Bear, M.F. (1995). Co-regulation of long-term potentiation and experience-dependent synaptic plasticity in visual cortex by age and experience. Nature *375*, 328–331.

Kirkwood, A., Silva, A., and Bear, M.F. (1997). Age-dependent decrease of synaptic plasticity in the neocortex of αCaMKII mutant mice. Proc. Natl. Acad. Sci. USA *94*, 3380–3383.

Komatsu, Y. (1983). Development of cortical inhibition in kitten striate cortex investigated by a slice preparation. Dev. Brain Res. *8*, 136–139.

Liu, X.B., and Jones, E.G. (1996). Localization of alpha type II calcium calmodulin-dependent protein kinase at glutamatergic but not gamma-aminobutyric acid (GABAergic) synapses in thalamus and cerebral cortex. Proc. Natl. Acad. Sci. USA *93*, 7332–7336.

Lo, D.C. (1995). Neurotrophic factors and synaptic plasticity. Neuron *15*, 979–981.

Lohof, A.M., Ip, N.Y., and Poo, M.M. (1993). Potentiation of developing neuromuscular synapses by the neurotrophins NT-3 and BDNF. Nature *363*, 350–353.

Luhmann, H.J., and Prince, D.A. (1991). Postnatal maturation of the GABAergic system in rat neocortex. J. Neurophysiol. *65*, 247–263.

Maffei, L., Berardi, N., Domenici, L., Parisi, V., and Pizzorusso, T. (1992). Nerve growth factor (NGF) prevents the shift in ocular dominance distribution of visual cortical neurons in monocularly deprived rats. J. Neurosci. *12*, 4651–4662.

Martin, D.L., and Rimvall, K. (1993). Regulation of gamma-aminobutyric acid synthesis in the brain. J. Neurochem. *60*, 395–407.

Marty, S., Carroll, P., Cellerino, A., Castren, E., Staiger, V., Thoenen, H., and Lindholm, D. (1996). Brain-derived neurotrophic factor promotes the differentiation of various hippocampal nonpyramidal neurons, including Cajal-Retzius cells, in organotypic slice cultures. J. Neurosci. *16*, 675–687.

Marty, S., Berzaghi, M., and Berninger, B. (1997). Neurotrophins and activity-dependent plasticity of cortical interneurons. Trends Neurosci. *20*, 198–202.

Mayford, M., Wang, J., Kandel, E.R., and O'Dell, T.J. (1995). CaMKII regulates the frequency-response function of hippocampal synapses for the production of both LTD and LTP. Cell *81*, 891–904.

McAllister, A.K., Lo, D.C., and Katz, L.C. (1995). Neurotrophins regulate dendritic growth in developing visual cortex. Neuron *15*, 791–803.

Micheva, K.D., and Beaulieu, C. (1997). Development and plasticity of the inhibitory neocortical circuitry with an emphasis on the rodent barrel field cortex: a review. Can. J. Physiol. Pharmacol. *75*, 470–478.

Mower (1991). The effect of dark rearing on the time course of the critical period in cat visual cortex. Brain Res. Dev. Brain Res. *58*, 151–158.

Nawa, H., Pelleymounter, M.A., and Carnahan, J. (1994). Intraventricular administration of BDNF increases neuropeptide expression in newborn rat brain. J. Neurosci. *14*, 3751–3765.

Patterson, S.L., Grover, L.M., Schwartzkroin, P.A., and Bothwell, M. (1992). Neurotrophin expression in rat hippocampal slices: a stimulus paradigm inducing LTP in CA1 evokes increases in BDNF and NT-3 mRNAs. Neuron *9*, 1081–1088.

Perkins, A.T., and Teyler, T.J. (1988). A critical period for long-term potentiation in the developing rat visual cortex. Brain Res. *439*, 222–229.

Porciatti, V., Pizzorusso, T., and Maffei, L. (1999). The visual physiology of the wild-type mouse determined with pattern VEPs. Vision Res., in press.

Reetz, A., Solimena, M., Matteoli, M., Folli, F., Takei, K., and De, C.P. (1991). GABA and pancreatic beta-cells: colocalization of glutamic acid decarboxylase (GAD) and GABA with synaptic-like microvesicles suggests their role in GABA storage and secretion. EMBO J. *10*, 1275–1284.

Reiter, H.O., and Stryker, M.P. (1988). Neural plasticity without postsynaptic action potentials: less-active inputs become dominant when kitten visual cortical cells are pharmacologically inhibited. Proc. Natl. Acad. Sci. USA *85*, 3623–3627.

Riddle, D., Lo, D.C., and Katz, L. (1995). NT-4-mediated rescue of lateral geniculate neurons from effects of monocular deprivation. Nature *378*, 189–191.

Rutherford, L.C., DeWan, A., Lauer, H.M., and Turrigiano, G.G. (1997). Brain-derived neurotrophic factor mediates the activity-dependent regulation of inhibition in neocortical cultures. J. Neurosci. *17*, 4527–4535.

Rutherford, L.C., Nelson, S., and Turrigiano, G.G. (1998). BDNF has opposite effects on the quantal amplitude of pyramidal neuron and interneuron excitatory synapses. Neuron. *21*, 521–530.

Sambrook, J., Fritsch, E.F., and Maniatis, T. (1989). Molecular Cloning: A Laboratory Manual (Cold Spring Harbor, NY: Cold Spring Harbor Laboratory Press).

Sheng, M., Cummings, J., Roldan, L.A., Jan, Y.N., and Jan, L.Y. (1994). Changing subunit composition of heteromeric NMDA receptors during development of rat cortex. Nature *368*, 144–147.

Shi, Y., Veit, B., and Baekkeskov, S. (1994). Amino acid residues 24–31 but not palmitoylation of cysteines 30 and 45 are required for membrane anchoring of glutamic acid decarboxylase, GAD65. J. Cell Biol. *124*, 927–934.

Sillito, A.M. (1979). Inhibitory mechanisms influencing complex cell orientation selectivity and their modification at high resting discharge levels. J. Physiol. (Lond.) *289*, 33–53.

Thoenen, H. (1995). Neurotrophins and neuronal plasticity. Science *270*, 593–598.

Wang, T., Xie, K., and Lu, B. (1995). Neurotrophins promote maturation of developing neuromuscular synapses. J. Neurosci. *15*, 4796–4805.

Widmer, H.R., and Hefti, F. (1994). Stimulation of GABAergic neuron differentiation by NT-4/5 in cultures of rat cerebral cortex. Brain Res. Dev. Brain Res. *80*, 279–284.

Wolff, J.R., Bottcher, H., Zetzsche, T., Oertel, W.H., and Chronwall, B.M. (1984). Development of GABAergic neurons in rat visual cortex as identified by glutamate decarboxylase-like immunoreactivity. Neurosci. Lett. *47*, 207–212.

Yan, Q., Rosenfeld, R.D., Matheson, C.R., Hawkins, N., Lopez, O.T., Bennett, L., and Welcher, A.A. (1997). Expression of brain-derived neurotrophic factor protein in the adult rat central nervous system. Neuroscience *78*, 431–448.